63 3 2

THERMAL STRESSES DUE TO LARGE SPANWISE TEMPERATURE GRADIENTS IN LONG THIN PLATES
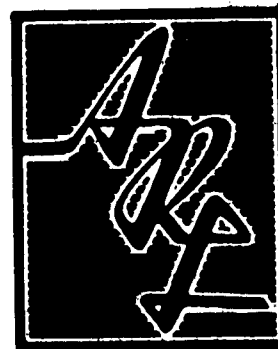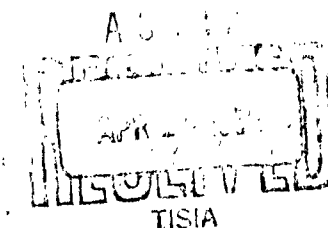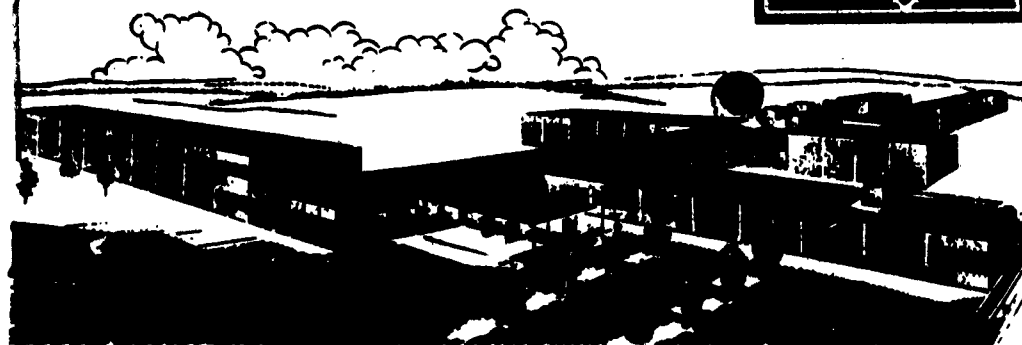
B. E. GATEWOOD
R. G. DALE
A. R. GLASER

THE OHIO STATE UNIVERSITY
COLUMBUS, OHIO

JANUARY 1963

TISIA

AERONAUTICAL RESEARCH LABORATORIES
OFFICE OF AEROSPACE RESEARCH
UNITED STATES AIR FORCE

401 505

NOTICES

Aeronautical Research Laboratories, Wright
Patterson AFB, Ohio. THERMAL STRESSES
DUE TO LARGE SPANWISE TEMPERATURE
GRADIENTS IN LONG THIN PLATES by B. E.
Gatewood, R. G. Dale, A. R. Glaser, The
Ohio State University, Columbus, O., Jan
uary1963. 62 p. incl. illus.(project 7063:
Task 7063-02) (Contract AF 33(616)-8330)
(ARL 63-4)   Unclassified Report

This report contains the results of a theoret-
ical and experimental investigation of the
thermal strains and stresses produced in un-
restrained long thin rectangular plates by
large spanwise temperature gradients. The
temperature distribution is steady state and
the stress distribution approximates the two-
dimensional "plane stress" solution of elas-

(over)

ticity theory. Two temperature gradients
were investigated, one of which the tempera-
ture changed about 150°F over a five-inch
distance and one in which the temperature
changed about 700°F over a one-inch distance.
It was found that for these relative large
temperature gradients the solutions for the
thermal stresses given in the literature were
either not applicable or impractical because
of the large number of terms required in the
series type solutions. By converting one of
the available Fourier Series solutions into a
Fourier Integral and using residues and super
position it is possible to construct a solution
for the stresses in which only a few terms
are needed in the series for the residues. The
calculated thermal strains compare reasona-
bly well with the experimental results, altho
there is considerable scatter in the strain
gage results on the tests.

THERMAL STRESSES DUE TO LARGE SPANWISE
TEMPERATURE GRADIENTS IN LONG THIN PLATES

B. E. GATEWOOD
R. G. DALE
A. R. GLASER

THE OHIO STATE UNIVERSITY
COLUMBUS, OHIO

JANUARY 1963

FOREWORD

This interim technical report was prepared by the Department of Aeronautical and Astronautical Engineering, The Ohio State University, on Contract AF 33(616)-833C for the Aeronautical Research Laboratories, Office of Aerospace Research, United States Air Force. The work reported herein was accomplished on Task 7063-02, "Research in the Mechanics of Structures" of Project 7063, "Mechanics of Flight", under the cognizance of Mr. Charles A. Davies of the Thermo-Mechanics Research Laboratory, ARL. The results contained herein were obtained during the period from 1 September 1961 to 1 August 1962.

ABSTRACT

This report contains the results of a theoretical and experimental investigation of the thermal strains and stresses produced in unrestrained long thin rectangular plates by large spanwise temperature gradients. The temperature distribution is steady state and the stress distribution approximates the two-dimensional "plane stress" solution of elasticity theory. Two temperature gradients were investigated, one in which the temperature changed about $150°F$ over a five-inch distance and one in which the temperature changed about $70°F$ over a one-inch distance. It was found that for these relative large temperature gradients the solutions for the thermal stresses given in the literature were either not applicable or impractical because of the large number of terms required in the series type solutions. By converting one of the available Fourier Series solutions into a Fourier Integral and using residues and superposition it is possible to construct a solution for the stresses in which only a few terms are needed in the series for the residues. The calculated thermal strains compare reasonably well with the experimental results, although there is considerable scatter in the strain gage results on the tests.

TABLE OF CONTENTS

LIST OF ILLUSTRATIONS

LIST OF ILLUSTRATIONS (CONTINUED)

INTRODUCTION

The problem of calculating the thermal stresses in plates subjected to temperature changes has received considerable attention in the literature. Solutions have been obtained under various assumptions as to the temperature distribution, stress distribution, and geometry of the plate. There are solutions for thin plates, thick plates, moderately thick plates, beam type plates with plane sections, slowly varying temperatures along plate, any temperature distribution with a Fourier Series expansion, etc. The question is which solutions are applicable to a given problem, which solutions can be obtained by a practical amount of calculation, and which solutions agree with experimental results for an actual plate.

To identify the various solutions and their associated assumptions and to specify the particular plate problem to be discussed in this report, consider the rectangular plate shown in Figure 1 with length 2L, width 2c, and thickness 2h. Let the plate be unrestrained
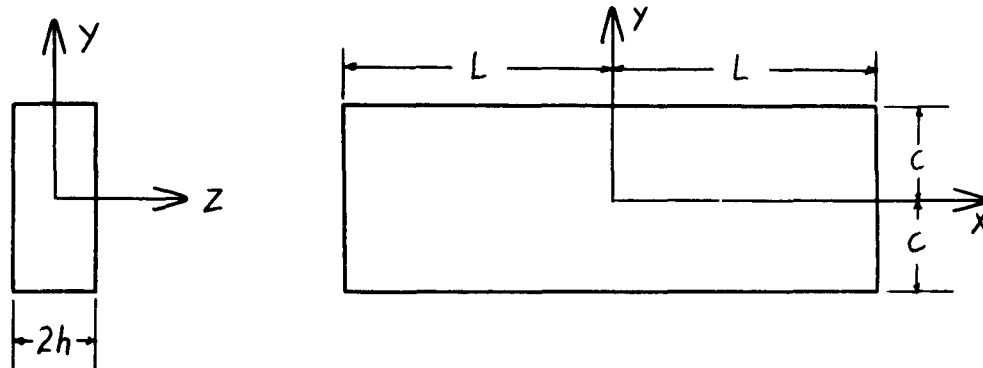
Fig. 1. Rectangular Plate Geometry

with no external loads so that the boundary conditions on the stresses are

$$\sigma_{xx} = \sigma_{xy} = \sigma_{xz} = 0 \quad \text{on the ends} \quad x = \pm L \tag{1}$$

$$\sigma_{yy} = \sigma_{xy} = \sigma_{yz} = 0 \quad \text{on the edges} \quad y = \pm c \tag{2}$$

$$\sigma_{zz} = \sigma_{xz} = \sigma_{yz} = 0 \quad \text{on the surfaces} \quad z = \pm h \tag{3}$$

where σ_{xx}, σ_{yy}, and σ_{zz} are the normal stresses in the x, y, z directions, respectively, and σ_{xy}, σ_{xz}, σ_{yz} are the shear stresses.

1

Let the plate be subjected to a temperature distribution T(x,y,z), which represents the change in temperature. The problem is to find the thermal stresses in the plate due to T(x,y,z). In general these stresses must satisfy the general equations of thermoelasticity theory:

$$\sum_{j=1}^{3} \frac{\partial X_{ij}}{\partial X_j} = 0 \qquad i = 1,2,3 \tag{4}$$

$$\nabla^2 X_{ij} + \frac{1}{1+v} \frac{\partial^2 \theta}{\partial X_i \partial X_j} = -\frac{\alpha E}{1-v} \nabla^2 T \, \delta_{ij} - \frac{\alpha E}{1+v} \frac{\partial^2 T}{\partial X_i \partial X_j} \tag{5}$$

where i,j = 1,2,3, $X_{11} = \sigma_{xx}$, $X_{22} = \sigma_{yy}$, $X_{33} = \sigma_{zz}$, $X_{12} = \sigma_{xy}$, $X_{13} = \sigma_{xz}$, $X_{23} = \sigma_{yz}$, $X_1 = x$, $X_2 = y$, $X_3 = z$, v is Poisson's ratio, E is modulus of elasticity, α is coefficient of thermal expression, δ_{ij} is Kronecker delta, and

$$\theta = \sigma_{xx} + \sigma_{yy} + \sigma_{zz} \quad ; \qquad \nabla^2 \theta = -\frac{2\alpha E}{1-v} \nabla^2 T \tag{6}$$

No solution of the general thermoelastic equations (1) - (6) has been obtained for general values of L, c, h, and T(x,y,z). However, various solutions of these equations have been obtained under certain simplifying assumptions. The classical two-dimensional plane stress problem is obtained by assuming the plate thickness 2h small compared to 2c and 2L and taking $\sigma_{zz} = 0$, $\sigma_{xz} = 0$, $\sigma_{yz} = 0$. For this plane stress case, the stresses can be expressed in terms of a stress function $\phi(x,y)$ satisfying the equation

$$\nabla^4 \phi + \alpha E \nabla^2 T = 0$$

with $\sigma_{xx} = \frac{\partial^2 \phi}{\partial Y^2}$, $\sigma_{yy} = \frac{\partial^2 \phi}{\partial X^2}$, $\sigma_{xy} = -\frac{\partial^2 \phi}{\partial X \partial Y}$

The two boundary conditions on ϕ are determined by Eqs. (1) and (2).

Basically, there are two objections to using the two-dimensional plane stress solutions as an approximation for the three-dimensional exact theory even when the plate is supposedly thin. One objection is that some of the compatibility equations

2

(Eq. 5) and one boundary condition at the edges and ends of the plate must be neglected in reducing the three-dimensional theory to the two-dimensional. This problem has been examined recently in Ref. 18 for the load case, where a systematic derivation from the exact theory of the differential equations and boundary conditions of plane stress is given. A second objection is that the temperature gradient must be considered in defining how thin the plate is. This problem is pointed out in Ref. 6 where an effort was made to calculate the three-dimensional stresses by using a power series in the thickness of a moderately thick plate. For example, if $T = T_{om}$ sin ($\pi x/a$), then the ratio $\pi h/a$ determines whether the thickness effects can be neglected, and a two-dimensional solution used. A tentative criteria given in Ref. 6 for the division between two-dimensional and three-dimensional stress methods is

$$
\left.
\begin{array}{ll}
\dfrac{\pi h}{a} < 0.2 , & \text{2 dimensional} \\[20pt]
\dfrac{\pi h}{a} > 0.2 , & \text{3 dimensional}
\end{array}
\right\} \tag{8}
$$

However, this value is questionable since in Ref. 6 only two boundary conditions were used at the edges of the plate in obtaining the corrections to the two-dimensional stresses due to the thickness effects.

By making further assumptions with regard to the temperature distribution and the boundary conditions, so-called one-dimensional solutions for the thermal stresses can be obtained for the plate. Consider the following cases for both one-dimensional and two-dimensional solutions for specified types of temperature distributions.

1. CASE OF T = T(z)

If $h \ll c \approx L$ and $T = T(z)$, then the elastic thermal stresses in the plate are

$$
\sigma_{xx} = \sigma_{yy} = \frac{\alpha E}{1 - \nu} \left[-T(z) + \frac{1}{2h} \int_{-h}^{h} T(z)\,dz + \frac{3z}{2h^3} \int_{-h}^{h} z\,T(z)\,dz \right] \tag{9}
$$

$\sigma_{zz} = \sigma_{xy} = \sigma_{xz} = \sigma_{yz} = 0$

away from the ends and edges of the plate (see page 10 of Ref. 5, page 278 and page 401 of Ref. 3). By Saint-Venant's principle the end and edge effects might be expected to extend into the plate for a distance of the order of 2h. The stresses given by Eq. (9) have been calculated for various temperature distributions. See for example Chapter 4 and the references therein of Ref. 5, Ref. 15, Section 12.5 of Ref. 3.

The inelastic problem for this case can be solved by the method of Ref. 8 using the stress-strain curves of the material at temperature. See Ref. 14 for a case of plastic flow in the plate.

Apparently no solution is available for the stresses near the ends and edges of the plate. Any solution for this case would be three-dimensional, involving all the six stresses.

2. CASE OF T = T(y)

If h ≪ c ≪ L and T = T(y) then the plate acts somewhat as a beam with the elastic thermal stresses given by

$$\sigma_{xx} = \alpha E \left[-T(y) + \frac{1}{2c} \int_{-c}^{c} T(y)\, dy + \frac{3y}{2c^3} \int_{-c}^{c} y\, T(y)\, dy \right] \tag{10}$$

$$\sigma_{yy} = \sigma_{zz} = \sigma_{xy} = \sigma_{xz} = \sigma_{yz} = 0$$

away from the ends (see page 9 of Ref. 5). To avoid possible thickness effects from large gradients, the further restriction from Eq. (8), (T = T_{0m} sin $\pi y/b$),

$$\frac{\pi h}{b} \leq 0.2 \tag{11}$$

should be used (Ref. 6). The end effects may extend into the plate about 2c by Saint-Venant's principle. However, if b < c this distance may be of the order of 2b.

For the end effects and for the case of c ≈ L, the problem becomes a two-dimensional plane stress problem (see Refs. 1, 9, 12, and Section 9-3 of Ref. 5). For end effects and for thickness effects, the problem becomes three-dimensional (see Ref. 6 for some work on this problem for moderately thick plates).

The inelastic problem for this case is covered in Ref. 8 using the stress-strain curves of the material at temperature.

3. CASE OF T = T(x)

If h ≪ c ≪ L and T = T(x) then the plate acts somewhat as a beam and on the basis of elementary strength of materials theory no thermal stresses are produced. Actually, the thermal stresses depend upon the gradient of T(x). To avoid possible thickness effects assume the condition in Eq. (8) is satisfied.

If the gradients are not too steep then the solution by Boley in Ref. 2 applies (see Ref. 7 for terms through the ninth derivative).

$$\frac{\sigma_{yy}}{\alpha E} = (y^2 - c^2)^2 \left[-\frac{1}{24} \frac{d^4 T}{d X^4} + \frac{1}{360} (y^2 - 3c^2) \frac{d^6 T}{d X^6} + \cdots \right]$$

$$\frac{\sigma_{xx}}{\alpha E} = -\frac{1}{6} (3y^2 - c^2) \frac{d^2 T}{d X^2} + \frac{1}{180} (15 y^4 - 30 y^2 c^2 + 7 c^4) \frac{d^4 T}{d X^4} + \cdots$$

$$\frac{\sigma_{xy}}{\alpha E} = y (y^2 - c^2) \left[\frac{1}{6} \frac{d^3 T}{d X^3} + \frac{1}{180} (7 c^2 - 3 y^2) \frac{d^5 T}{d X^5} + \cdots \right]$$

(12)

If

$$T = T_{om} \sin \frac{m \pi X}{d} \qquad (13)$$

then

$$\frac{d^p T}{d X^p} = \pm T \left(\frac{m \pi}{d} \right)^p \quad \text{p even}$$

in Eq. (12) so that $m\pi/a$ must be considerably less than one for Eq. (12) to be useful. Note that the series in Eq. (12) terminates if T is expressed in a polynomial. This solution does not apply at the ends.

If the temperature is expanded into a Fourier series such as

$$T(X) = T_R + \sum_{m=1}^{\infty} T_m \sin \lambda_m X \; ; \; \lambda_m = \frac{m \pi}{L} \qquad (14)$$

then the stresses can be obtained from Timoshenko and Goodier (pages 48 and 405 of Ref. 13)

$$\sigma_{xx} = -2\alpha E \sum K_{1m} T_m \sin \lambda_m X$$

$$\sigma_{yy} = 2\alpha E \sum \left[K_{2m} - \frac{1}{2} \right] T_m \sin \lambda_m X$$

$$\sigma_{xy} = 2\alpha E \sum K_{3m} T_m \cos \lambda_m X$$

(15)

5

where

$$K_{2m} = \left\{ \frac{(\lambda_m C \; COSH\lambda_m C \mp SINH\lambda_m C) COSH\lambda_m Y}{SINH \; 2\lambda_m C + 2\lambda_m C} \right.$$

$$\left. - \frac{\Delta_m Y SINH\lambda_m Y SINH\lambda_m C}{SINH \; 2\lambda_m C + 2\lambda_m C} \right\}$$

$$K_{3m} = \left\{ \frac{\Delta_m C COSH\lambda_m C \; SINH\lambda_m Y}{SINH \; 2\lambda_m C + 2\lambda_m C} \right.$$

$$\left. - \frac{\Delta_m Y COSH\lambda_m Y SINH\lambda_m C}{SINH \; \lambda_m C2 + 2\lambda_m C} \right\} \qquad (16)$$

It has been shown in Ref. 7 that the solution in Eq. (12) can be obtained directly from Eq. (15) by expanding the hyperbolic functions in Eq. (16) in power series and collecting terms on powers of λ_m. This solution does not apply at the ends.

Horvay in Refs. 4 and 10 gives two-dimensional solutions for a step change in the temperature. Since the infinite gradient at the step does not satisfy Eq. (8), there is a question of the thickness effects in a range of ± 2h or more spanwise on either side of the step.

Przemieniecki in Ref. 12 and Horvay in Refs. 4 and 9 include the end effects in two-dimensional solutions. End effects are also included in the method used in Ref. 1. For these solutions h ≪ c ≈ L relations among h, c, and L can be used. Przemieniecki's procedure (Ref. 12) involves a double series giving

$$\sigma_{xx} = \left(\frac{1}{2C} \right)^2 \sum_m \sum_n A_{mn} \; \phi_m(\xi) \; \phi_n''(\eta)$$

$$\sigma_{yy} = \left(\frac{1}{2L} \right)^2 \sum_m \sum_n A_{mn} \; \phi_m''(\xi) \; \phi_n(\eta) \qquad (17)$$

$$\sigma_{xy} = -\frac{1}{4LC} \sum_m \sum_n A_{mn} \; \phi_m'(\xi) \; \phi_n'(\eta)$$

where

$$\xi = \frac{1}{2}\left(1 + \frac{x}{L} \right) \quad ; \quad \eta = \frac{1}{2}\left(1 + \frac{y}{C} \right)$$

6

with

$$\phi_m(\xi) = \cosh\beta_m \xi - \cos\beta_m \xi - \gamma_m(\sinh\beta_m \xi - \sin\beta_m \xi) \tag{18}$$

$$\gamma_m = \frac{\cosh\beta_m - \cos\beta_m}{\sinh\beta_m - \sin\beta_m}$$

$\beta_1 = 4.730041$	$\gamma_1 = 0.982502$
$\beta_2 = 7.853205$	$\gamma_2 = 1.000777$
$\beta_3 = 10.995608$	$\gamma_3 = 0.999967$
$\beta_4 = 14.137166$	$\gamma_4 = 1.000002$
$\beta_5 = 17.278760$	$\gamma_5 = 1.000000$

$$\beta_m = \frac{2m+1}{2}\pi \quad ; \quad \gamma_m = 1.000000 \quad ; \quad m > 5$$

$$A_{mn} + \frac{2(L/C)^2}{\beta_m^4 + (L\beta_m/C)^4}\sum_{p}^{\infty}\sum_{q}^{\infty} A_{pq}\, C_{pm}\, C_{qn} = \frac{(2L)^4 b_{mn}}{\beta_m^4 + (L\beta_m/C)^4} \tag{19}$$

$$C_{pm} = 8\beta_p^2\beta_m^2\, \frac{\gamma_m\beta_m - \gamma_p\beta_p}{\beta_m^4 - \beta_p^4} \quad ; \quad p \neq m$$

$$C_{pm} = \gamma_m\beta_m[2 - \gamma_m\beta_m] \quad ; \quad p = m$$

$$b_{mn} = -\alpha E \int_0^1\int_0^1 \nabla^2 T\, \phi_m(\xi)\, \phi_n(\eta)\, d\xi\, d\eta \tag{20}$$

The functions $\phi_m(\xi)$ in Eq. (18) together with the corresponding functions $\phi_m(\eta)$ are the characteristic functions of a vibrating beam with fixed ends satisfying $\phi = \phi' = 0$ at the ends $\xi = 0$ and 1 for $\phi_m(\xi)$ and $\eta = 0$ and 1 for $\phi_m(\eta)$. Thus the use of these functions in Eq. (17) allows all boundary conditions on the stresses (eq. (1, 2)) to be satisfied.

If the temperature distribution has a form such as that in Eq. (13), then the magnitude of the terms given by Eq. (20) depends upon the ratio $(m\pi/a)^2$ from Eq. (13), and this in turn dictates the number of terms needed in Eqs. (17) and (19) to get the thermal stresses within the desired accuracy. If the temperature gradient is

large, as might be indicated by a value of $m\pi/a > 1$, then it is possible that a large number of A_{mn} terms will be needed to get the stresses.

4. CASE OF T = T(x,y)

In Ref. 2 Boley gives a solution corresponding to Eq. (12) for T = T(x,y). As indicated by Eq. (20) above, Przemieniecki's solution in Ref. 12 can be used for T = T(x,y). Again the magnitude of the temperature gradients in either or both directions would affect the applicability of these solutions.

5. CASE OF T = T(x,y,z)

Some discussion of this case with the temperature a polynomial in z is given in Ref. 6 (see also the references given in Ref 6). No general solutions for this case are available.

From the above discussion it is evident that there is considerable work, both experimental and theoretical, to be done to clarify presently available solutions of the plate problem, to develop further solutions for ranges of certain parameters where present solutions may not apply, and to solve certain cases for which no solutions have been developed.

The purpose of this report is to initiate some theoretical and experimental work in an effort to clarify some of the questions raised in the above discussion. The work in this report is restricted to the two-dimensional case--that is, the temperature gradients considered are such that Eq. (8) holds for the two-dimensional case. Thus, it is expected that the thickness effects will be small. No effort will be made to clarify the third boundary condition problem arising in reducing from the three-dimensional case to the two-dimensional case. Since most of the work reported in the literature, both theoretical and experimental, has been on cases 1 and 2, T = T(z) and T = T(y), the effort in this report is devoted to case 3, T = T(x). There appears to be little, if any, experimental work for case 3, and there are questions as to the applicability of the theoretical solutions for relatively large temperature gradients. Two steady state temperature distributions are used, one with a medium gradient and one with a relatively steep gradient, approaching the border line between the two cases in Eq. (8). Equation (12) cannot be used for either temperature distribution, while Eqs. (15) and (17) can be used for the medium gradient case, but not for the steep gradient case.

CALCULATION PROCEDURES

This section describes the procedures for calculating the thermal stresses in a rectangular plate for two different steady state spanwise temperature distributions. These temperature distributions correspond to those obtained in experiments on a plate with 2L = 48", 2c = 9", and 2h = 1/4". In one case an approximate cosine wave with a twelve inch wavelength was produced in the plate and in the other case a narrow hot region about three inches wide was produced at the middle of the plate.

A. FOUR WAVE CASE

In this case a temperature distribution of the form

$$T = T_R - T_o \cos(4\pi x/L) \tag{21}$$

was produced approximately in the plate. For such a temperature distribution the thermal stresses away from the ends of the plate can be calculated directly from Eq. (15) using one term of a cosine series rather than the sine series given in Eq. (15). However, this solution does not apply near the ends of the plate. To obtain the stresses near the ends and to investigate how far the end effects extend into the plate, Przemieniecki's solution (Ref. 12) given in Eq. (17) was used. Again, for the temperature distribution in Eq. (21), it was an easy matter to calculate the b_{mn} coefficients in Eq. (20). But then the question is how many terms are needed in the double series in Eq. (17) to obtain accurate thermal stresses. To investigate the number of required terms, Eq. (19) was solved by matrices for eight A_{mn} constants and for fifty A_{mn} constants. In the latter case m took odd values from 1 to 19 and n odd values from 1 to 9.

To calculate the stresses from Eq. (17) using the A_{mn} constants it is necessary to modify the function $\phi_m(\xi)$ in Eq. (18) to avoid the subtraction of extremely large numbers for large values of m. Since approximately for all β_m

$$SIN\beta_m \approx (-1)^m \quad , \quad COS\beta_m \approx 0$$

$$\gamma_m \approx 1 + 2(-1)^m e^{-\beta_m} \quad , \quad e^{-2\beta_m} \approx 0$$

Eq. (18) can be written as

$$\left.\begin{aligned}
\phi_m(\xi) &= \tfrac{1}{2} e^{\beta_m \xi}(1-\gamma_m) + \tfrac{1}{2} e^{-\beta_m \xi}(1+\gamma_m) - COS\beta_m \xi + \gamma_m SIN\beta_m \xi \\[8pt]
&= -(-1)^m e^{-\beta_m(1-\xi)} + e^{-\beta_m \xi} + (-1)^m e^{-\beta_m(1+\xi)} - COS\beta_m \xi \\[8pt]
&\quad + SIN\beta_m \xi + 2(-1)^m e^{-\beta_m} SIN\beta_m \xi
\end{aligned}\right\} \tag{22}$$

9

Further, $e^{-\beta_1} \approx 0.009 > e^{-\beta_m}$ for all m so that with the approximation $e^{-\beta_m} = 0$ Eq. (22) becomes

$$\phi_m(\xi) = -(-1)^m e^{-\beta_m(1-\xi)} + e^{-\beta_m \xi} + \sqrt{2} \, SIN(\beta_m \xi - \tfrac{\pi}{4}) \tag{23}$$

Also, neglecting $e^{-\beta_1}$, Eq. (23) can be further reduced for ξ away from the ends of the plate so that

$$\phi_m(\xi) = \sqrt{2} \, SIN(\beta_m \xi - \tfrac{\pi}{4}) \quad , \quad \frac{\delta_1}{\beta_m} \leq \xi \leq 1 - \frac{\delta_1}{\beta_m} \tag{24}$$

If m > 3 in Eq. (24), then the range of ξ for which Eq. (24) is applicable covers most of the plate. Also, for m > 3, only one of the exponential terms in Eq. (23) is needed on either end, the two ends being the same except possibly for sign.

Using Eqs. (23) and (24) and the tables of Ref. 16 the $\phi_m(\xi)$ and $\phi_n(\eta)$ functions were evaluated for L/c = 48/9 and for several values of η at $\xi = 0.125$ or x/L = -0.75 and $\xi = 0.375$ or x/L = -0.25. With these values the stresses in Eq. (17) were calculated using eight A_{mn} constants and using fifty A_{mn} constants. It was found that about seventeen of the fifty constants contributed significantly to the σ_{yy} stress, while about twenty-five contributed to σ_{xx}, and that the results given by these constants differed by a considerable amount from those given by the eight constants (as much as fifteen per cent variation at some points).

The results for σ_{xx} and σ_{yy} given by the seventeen and twenty-five constants, respectively, in Eq. (17) are compared to the results given by Timoshenko's long plate solution (Eq. 15) in Figs. 2 and 3. In Fig. 3 the distance from the end of the plate is twice the plate width while in Fig. 2 the distance from the end is two-thirds of the plate width. By Saint-Venant's principle it would be expected that the agreement between the two solutions would be better for the case of Fig. 3, as it is. However, for the case of Fig. 2, the agreement appears to be better than might be expected. This may be due to the temperature gradient in this case. The temperature changes from its minimum value at the plate end to its maximum value at the x/L = -0.75 location used in Fig. 2, thus causing the thermal stresses to be approximately zero at a point only one-third of the plate width from the end of the plate. Due to these large stress changes in a short distance, it is possible the end effects may not extend as far into the plate as they may for small spanwise temperature gradients.

B. CASE OF THREE INCH HOT REGION (SHORT WAVE CASE)

From Eq. (14) it is evident that the representation of a three-inch wide temperature hump of large amplitude in the middle of a 48-inch long plate by a Fourier series requires a large number of terms--one of the largest terms corresponds to m = 16. The large number of terms requires a prohibitive amount of calculation to

obtain the stresses in Eq. (15). Due to the second derivative of T in Eq. (20) and the double series in Eq. (17), it appears that a still larger number of terms would be required in Eqs. (20) and (19) to evaluate the A_{mn} constants for Przemieniecki's solution (Eq. 17).

It is possible to reduce the amount of calculation by converting the Fourier Series solution in Eq. (15) to a Fourier integral. Since the temperature distribution in the narrow hot region is determined by measurement it is simpler to represent the temperature distribution by a sum of rectangles (see Fig. 18) and hence determine the Fourier integral solution for a rectangular distribution. Consider the rectangular element shown in Fig. 4.
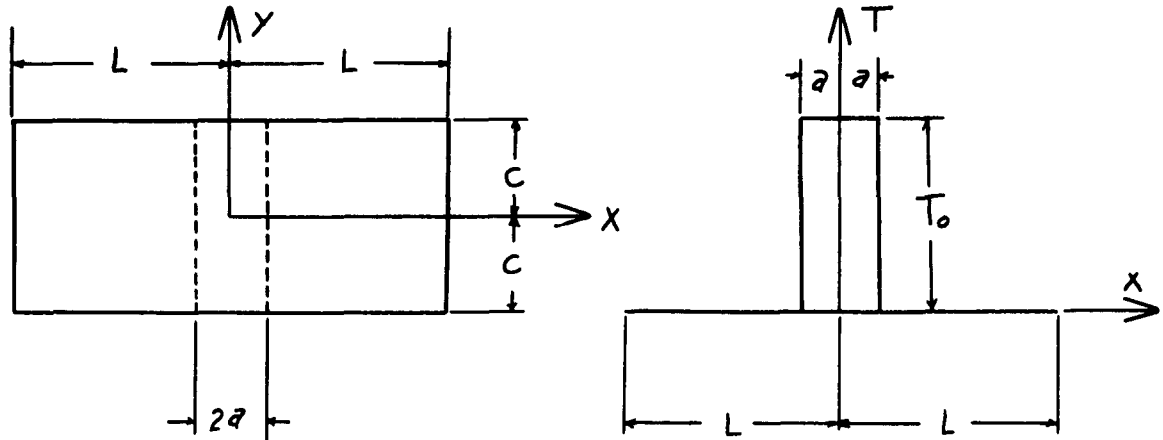
Figure 4. Rectangular Element for Temperature Distribution

This temperature variation can be represented by

$$T = \sum_{n=0}^{\infty} T_n \cos \lambda \gamma t_n$$

where

$$T_n = \frac{2 C T_o}{L t_n} \sin \lambda t_n ; \quad t_n = \frac{n \pi}{L} C ; \quad \lambda = \frac{a}{c} ; \quad \gamma = \frac{x}{a}$$

(25)

11

Timoshenko and Goodier give the solution (Eq. (15)) for $T = T_m \cos(t_m \lambda \psi)$ as

$$(\sigma_{xx}/\alpha E)_m = -2 T_m K_{1m}(t_m, \eta) \cos t_m \lambda \psi$$

$$(\sigma_{yy}/\alpha E)_m = 2 T_m [K_{2m}(t_m, \eta) - \tfrac{1}{2}] \cos t_m \lambda \psi$$

(15A)

where

$$K_{\substack{1\\2}m} = \frac{(t_m \cosh t_m \mp \sinh t_m)\cosh \eta t_m}{2t_m + \sinh 2t_m} - \frac{2 t_m \sinh t_m \sinh \eta t_m}{2 t_m + \sinh 2 t_m}$$

(16A)

and

$$\eta = \frac{y}{c}$$

Therefore for the temperature profile under investigation

$$\sigma_{xx}/\alpha E = \sum_{m=0}^{\infty} -2 T_m K_{1m}(t_m, \eta)\cos \lambda \psi t_m$$

$$\sigma_{yy}/\alpha E = \sum_{m=0}^{\infty} 2 T_m [K_{2m}(t_m, \eta) - \tfrac{1}{2}]\cos \lambda \psi t_m$$

(26)

Substitute Eq. (25) into Eq. (26) and let $\pi c/L = \Delta t$, whence

$$\sigma_{xx}/\alpha E T_o = -\frac{4}{\pi} \sum_{m=0}^{\infty} K_{1m}(t_m, \eta)\sin \lambda t_m \cos \lambda \psi t_m \frac{\Delta t}{t_m}$$

$$\sigma_{yy}/\alpha E T_o = \frac{4}{\pi} \sum_{m=0}^{\infty} [K_{2m}(t_m, \eta) - \tfrac{1}{2}]\sin \lambda t_m \cos \lambda \psi t_m \frac{\Delta t}{t_m}$$

(27)

12

or in the limit

$$\sigma_{xx}/\alpha E T_0 = -\frac{4}{\pi}\int_0^\infty K_1(t,\eta)\, SIN\, \lambda t\, COS\, \lambda \psi t\, \frac{dt}{t}$$

$$\sigma_{yy}/\alpha E T_0 = \frac{4}{\pi}\int_0^\infty [K_2(t,\eta) - \frac{1}{2}]\, SIN\, \lambda t\, COS\, \lambda \psi t\, \frac{dt}{t}$$

(28)

These integrals are evaluated by the method of residues in the APPENDIX so that

$$\sigma_{xx}/\alpha E T_0 = -4\sum_{\pi}^{\infty} f_{1n}(\eta) G_{1n}(\lambda, \psi) - f_{2n}(\eta) G_{2n}(\lambda, \psi)$$

and

$$\sigma_{yy}/\alpha E T_0 = 4\sum_{\pi}^{\infty} f_{3n}(\eta) G_{1n}(\lambda, \psi) - f_{4n}(\eta) G_{2n}(\lambda, \psi)$$

(29)

where analytical expressions for the functions $f_{1n}(\eta)$, $f_{2n}(\eta)$, $f_{3n}(\eta)$, $f_{4n}(\eta)$, $G_{1n}(\lambda,\psi)$, and $G_{2n}(\lambda,\psi)$, are given in the APPENDIX. Graphs of $f_{1n}(\eta)$, $f_{2n}(\eta)$, $f_{3n}(\eta)$, and $f_{4n}(\eta)$ for n = 1,2,3 are shown in Figures 5,6,7 and 8 respectively. Graphs of $G_{1n}(\lambda,\psi)$ and $G_{2n}(\lambda,\psi)$ with λ = 0.27775 are shown in Figures 9 and 10 respectively. Although this solution does not meet the conditions of a free end at x = ± L, the stresses at the ends are zero for a << L. By using various values of λ and T_0 and by shifting the origin it is possible to approximate a general temperature variation by a sum of rectangles and thus obtain the stresses by superposition from Eq. (29).

Note that the shear stress, σ_{xy}, can be evaluated in a similar way to σ_{xx} and σ_{yy} above.

The stresses shown in Figures 28, 29, and 30, corresponding to λ = 0.27775, were calculated using only three terms in Eq. (29) corresponding to the residues at the first three poles. It can be seen that convergence is poor near the step (i.e. near ψ = ± 1). At ψ = ± 1, and η = 0 the curves could easily be smoothed across the step as shown in Figure 28. At η = 1 in Figure 30 the stress gradient is quite large and there is considerable doubt as to the nature of the σ_{xx} stress variation across the step. Investigation of this large stress gradient would require the use of additional poles; the use of a high speed computer would be recommended since a considerable amount of work is necessary to evaluate the different functions at the different poles. However, in the superposition process used herein, this large jump is smoothed out and the smooth variation shown in Figure 33 is produced for the measured temperature distribution (see later discussion in Results section).

13

EXPERIMENTAL PROCEDURE

The test specimen was a piece of 2024-T3 bare aluminum alloy plate 0.25 inches thick machined as shown in Figure 1 with 2L = 48 in., 2c = 9 in., 2h = 0.25 in. The specimen was machined in such a manner as to reduce any residual stresses to a minimum. The 0.25 inch thickness was selected so that any temperature gradient through the thickness would be negligible.

The test specimen was heated by General Electric T-3 quartz lamps supported by radient heating reflector units models AU8-612 and AU5-212 and controlled by a Thermac three phase combined temperature controller and power regulator, model SPG 6266W.

Heat sinks were provided by means of the two types of cooling tubes shown in Figure 11 which permitted direct contact of the cooling water with the specimen. The cooling tube shown in Figure 11A was used to provide cooling for Case A, but it was found that even with water entering and leaving both ends of the tube there was some chordwise variation in the temperature. This was probably due to the fact that the water near the ends of the tube was in a more turbulent state than along the center of the plate providing less cooling of the plate center than the plate edges. This problem was reduced in Case B by use of the cooling tube shown in Figure 11B, where an internal tube with small holes sprayed water on the plate. Thermoflax shielding was used to protect certain regions of the plate from radiation and thus to control the length of the heat conduction path over these regions.

The desired temperature profiles were produced by properly positioning the heating lamps, cooling tubes, and shielding over and on the plate. The configurations used for Case A and Case B are shown in Figure 12A and 12B respectively. Although the heating lamps were on one side of the plate and the cooling tubes on the same side, the temperature variation through the thin plate was negligible.

The temperature of various points on the plate was determined by Constantan-Alumel thermocouples. The location of the thermocouples on the specimen for Case A and Case B is shown in Figure 13A and 13B. The temperature distributions obtained for several tests are shown in Figures 14, 15, 16, 17, 18. It can be seen from these figures that the temperature gradients produced for Case A were about 30°F per inch and for Case B was about 70°F per inch. These are steady-state temperature distributions; no transient state tests were run.

Strains were determined by means of high temperature metalfilm strain gages. The type used for Case A were Budd C12-142-B and for Case B were Budd C12-124-C. All gages were mounted with Armstrong A-12 cement with parts A and B mixed in a ratio of 2:1 for maximum hardness. Gages were mounted on the upper and lower surfaces and the edges of the plate as shown in Figure 13A for Case A and Figure 13B for the Case B. After all gages had been mounted on the plate, the plate was then temperature cycled a minimum of five times to properly "seat" and "shake down" the gages to obtain a repeatable apparent strain vs. temperature curve. Each strain gage circuit was then calibrated to obtain apparent strain vs. temperature curves.

The electrical circuitry used with this multiple strain gage installation is shown in Figures 19 and 20. The circuit shown in Figure 19 was used with Case A in which bending strains were electrically eliminated and a three-wire lead system was used. It was found that the three-wire system proved ineffective due to the physical arrangement of the lead wires. During tests, several gages were damaged which rendered certain circuits useless for subsequent tests and those data points were lost.

Since the three-wire lead system employed in Case A proved ineffective, this system was abandoned in Case B in order to increase the strain sensitivity of the circuit. The circuit shown in Figure 20 was used for Case B in which the gages on the upper and lower surfaces of the plate were monitored separately; bending strains could be eliminated by averaging the output of the upper and lower gages. Many of the gages were lost during test, however, because the limit temperature of the cement was once accidentally exceeded which caused many of the lead wire terminal posts to pull out and disconnect from the gages; also on the upper surface of the heated portion of the plate, the unexpected high radiation of the heating lamps caused the Teflon insulation of the lead wires and the 450°F solder connections of the lead wire to the terminal posts of melt. Consequently most of the data points in the heated portion of the plate were lost. Since there was obviously a tremendous temperature gradient through the bonding cement, the functioning gages on the upper surface of the plate in the heated portion recorded an excessive compressive strain, roughly of about 300 microinches per inch, which could not accurately be accounted for.

The strain distributions observed for Case A and Case B are discussed in the RESULTS section of this report.

RESULTS

A. FOUR WAVE CASE

The stresses calculated by Przemieniecki's method (Ref. 12) and shown graphically in Figures 2 and 3 are converted to strain and are shown in Figures 21, 22, and 23 along with the experimentally determined strains. It can be seen that more compressive strain was observed in all cases at the plate center ($\eta = 0.5$) than was predicted. This is believed due to uneven chordwise heating in which the center of plate was observed to be hotter than the edges, the temperature difference ranging between 15°F and 30°F, which was not accounted for in the theoretical calculations but which would cause more compression in the plate center than predicted.

The effect of differences in peak temperatures was also investigated. The strains observed due to the temperature variation shown in Figure 17 are shown in Figures 24, 25, and 26. It was concluded on the basis of these results (and later verified both analytically and experimentally when investigating Case B) that the effects of small differences in peak temperatures was essentially negligible a wave length away from the temperature peaks and could be ignored. The strains at the location of each peak temperature are determined by the corresponding peak temperature.

B. THREE INCH HOT REGION

The measured temperature at various points on the plate are shown in Figure 27. It can be seen that the symmetrical temperature distribution desired was not attained. Figure 18 shows the average spanwise temperature variation upon which the theoretical calculations are based. Figure 18 also shows the temperature steps used to approximate this temperature profile. Figures 28, 29, and 30 show the calculated stresses corresponding to a step with $\lambda = 0.27775$. A series of such graphs were constructed

with the various values of λ and used to calculate the stresses produced by the temperature distribution obtained. These stresses are shown in Figures 31, 32, and 33. The experimentally determined strains normalized with respect to αT_0 where T_0 is the maximum temperature difference, are also shown in Figs. 31, 32, and 33. The observed strains are presented in a table in Figure 34. Even though the test data is incomplete it can be seen that the correlation shown in Figure 31 is good and that the trend predicted by theory agrees with the data presented in Figure 34.

CONCLUSIONS AND RECOMMENDATIONS

Results obtained in this investigation of spanwise temperature gradients show that there are both theoretical and experimental difficulties when the gradients become large, requiring modification of existing procedures or development of new procedures. The temperature gradients investigated in Case A (Four Wave Case) were such that $\pi c/a \approx 3\pi/4$ and $\pi h/a \approx 0.06$ (see Eq. (8)). Since for $\pi c/a > 1$, the solution given by Boley (Eq. (12)) would involve an impractical number of terms, it was not used. The solutions given by Timoshenko (Eq. (15)) and Przemieniecki (Eq. (17)) were investigated. The question of convergence of Przemieniecki's solution was investigated by considering a rectangular array of 50 coefficients (A_{mn}'s) and determining which of these 50 terms were dominating. It was found that the dominating terms were determined principally by the temperature distribution and the component of stress sought. For the Four Wave Case it was necessary to use about seventeen terms for σ_{yy} and twenty-five terms for σ_{xx}. The solution obtained using Przemieniecki's method was then compared with Timoshenko's solution at $x/L = -0.25$ and $x/L = -0.75$. It was found that both methods were in good agreement at $x/L = -0.25$, which is 18 inches from the end of the 9-inch wide plate. Although Przemieniecki's method includes end effects and Timoshenko's method does not, good agreement was also found at $x/L = -0.75$ which is 6 inches away from the end of the 9-inch wide plate. This agreement is better than might be expected by Saint-Venant's principle and is probably due to the temperature gradient in this particular case. The temperature changes from its minimum value at the plate end to its maximum value at a point six inches from the end, thus causing the thermal stresses to be approximately zero at a point three inches from the end of the plate. The experimental results for both cases, 18 inches and 6 inches from the plate end agree quite well with the calculated results. No thickness effects appeared to be present in the test results.

The temperature gradients investigated in Case B (three-inch case) were such that $\pi c/a \approx 3\pi$ and $\pi h/a \approx 0.2$, thus bordering on the thickness effect problem (Eq. (8)). No conclusions could be drawn regarding thickness effects due to the nature of the recording mechanism and the recorded data. With a temperature gradient of this size existing only in the center section of the plate, Przemieniecki's method was abandoned due to the convergence problem. The series solution given by Timoshenko had to be modified by resorting to Fourier integrals and integration by residues before a practical means of stress determination away from the ends was obtained. The method presented herein is applicable to arbitrary spanwise temperature variations as long as the temperature variations occur away from the ends of the plate and thickness effects can be neglected.

It was found that the cooling system used in Case B proved to be an efficient means of providing a uniform line heat sink as long as the water is allowed to come

into direct contact with the surface to be cooled. The efficiency of this type cooling tube is decreased when strain gages and water-proofing compounds are introduced along the line of water contact.

It is recommended that a means of strain determination other than strain gages be investigated. It was found that under the conditions of test, especially with high temperature gradients, that the problems of strain gage installations are many. Among these are the problems of shorter gage lengths for high strain gradients, the effect of high radiation directly on the strain gages and the bonding cement, the problem of lead wire connections and insulation, the high mortality rate in installations of this size, "shake down" and proper calibration, and the effect of sudden heat surges as would be encountered in transient state tests.

It is also recommended that the case of $T = T(x,y)$ be studied, initially investigating the solution proposed by Przemieniecki to include end effects. Perhaps it would be possible to modify Przemieniecki's solution in a manner similar to the one used to modify Timoshenko's solution such that the problem of a large number of terms would be reduced or eliminated.

It is further recommended that the problem of thickness effects be investigated in the hope of establishing certain geometrical criteria which predict the degree to which thickness effects are present and thus establish a limit for two-dimensional theory.

17

REFERENCES

1. Becker, H., "Simplified Thermal Stress Analysis of Re-entry Structures," American Rocket Society paper No. 1692-61, April 1961.

2. Boley, B. A., "The Determination of Temperatures, Stresses, and Deflections in Two-Dimensional Thermoelastic Problems," Journal of Aeronautical Sciences, Vol. 23, pp. 67-75 (1956).

3. Boley, B. A., and Weiner, J. H., "Theory of Thermal Stresses," John Wiley and Sons, New York, 1960.

4. Born, J. S., and Horvay, G., "Thermal Stresses in Rectangular Strips - II," Journal of Applied Mechanics, Vol. 22, Sept. 1955, pp. 401-406.

5. Gatewood, B. E., "Thermal Stresses," McGraw-Hill Book Co., New York, 1957.

6. Gatewood, B. E., "Thermal Stresses in Moderately Thick Elastic Plates," Journal of Applied Mechanics, Vol. 26, pp. 432-436, 1959.

7. Gatewood, B. E., and Dale, R. G., "Note on Two Dimensional Stresses in Long Beams with Spanwise Variation of Load and Temperature," ARL 62-329, April 1962.

8. Gatewood, B. E., and Gehring, R. W., "Allowable Axial Loads and Bending Moments in Inelastic Structures Under Nonuniform Temperature Distribution," Journal of Aerospace Sciences, Vol. 29, p. 513-520, May 1962.

9. Horvay, G., "The End Problem of Rectangular Strips," Journal of Applied Mechanics, Vol. 20, March 1953.

10. Horvay, G., "Thermal Stresses in Rectangular Strips," Proceedings of the 2nd National Congress of Applied Mechanics, ASME, 1954, pp. 313-322.

11. Nelson, L. W., "Thermal Stresses Owing to a Hot Spot in a Rectangular Strip," Journal of Applied Mechanics, Vol. 26, Dec. 1959, pp. 488-490.

12. Przemieniecki, J. S., "Thermal Stresses in Rectangular Plates," The Aeronautical Quarterly, Vol. 10, pp. 65-78 (1959).

13. Timoshenko, S. and Goodier, J. N., "Theory of Elasticity," 2nd Ed. McGraw-Hill Book Co., New York, 1951.

14. Weiner, J. H., "An Elastic Plastic Thermal Stress Analysis of a Free Plate," WADC TN 55-512, ASTIA AD 97338, June 1955.

15. Weiner, J. H., and Mechanic, Harold, "Thermal Stresses in Free Heat Pulse Inputs," WADC TR 54-428, ASTIA AD 118156, March 1957.

16. Young, Dana, and Felgar, R. P., "Tables of Characteristic Functions Representing Normal Modes of Vibration of a Beam," University of Texas Publication, No. 4913; July 1949.

17. Seewald, F., Abhandl. Aerodynam. Inst., Tech. Hochschule, Aachen, Vol. 7, p. 11, 1927.

18. Reis, E. L., and Locke, S., "On the Theory of Plane Stress," Quarterly of Applied Mathematics, Vol. 19, Oct. 1961, p. 195-203.

APPENDIX

The details of the evaluation by the use of residues of the integrals referred to in the section on CALCULATION PROCEDURES is given below. The problem is to evaluate

$$\int_0^\infty SIN\,\lambda t\,COS\,\lambda\gamma t\,K_1(t,\gamma)\frac{dt}{t} \tag{A1}$$

$$\int_0^\infty SIN\,\lambda t\,COS\,\lambda\gamma t\,[K_2(t,\gamma)-\tfrac{1}{2}]\frac{dt}{t} \tag{A2}$$

where

$$K_{\frac{1}{2}}(t,\gamma)=\frac{(t\,COSH t\mp SINH t)COSH\gamma t-\gamma t\,SINH t\,SINH\gamma t}{SINH 2t+2t} \tag{A3}$$

Two relations to be used in the derivations are

$$\int_0^\infty SIN\,\lambda t\,COS\,\lambda\gamma t\,\frac{dt}{t}=\begin{bmatrix}0 & \text{for} & |\gamma|>1\\ \pi/4 & \text{for} & |\gamma|=1\\ \pi/2 & \text{for} & |\gamma|<1\end{bmatrix} \tag{A4}$$

and

$$SIN\,\lambda t\,COS\,\lambda\gamma t=\tfrac{1}{2}[SIN\,\lambda t(1+\gamma)+SIN\,\lambda t(1-\gamma)] \tag{A5}$$

From Eq. (A3)

$$K_1(t,1)=K_1(t,-1)=(2t-SINH2t)/(4t+2SINH2t)$$

$$K_2(t,1)=K_2(t,-1)=\tfrac{1}{2} \tag{A6}$$

20

whence

$$-\frac{1}{2} \leq K_1(t,1) < 0 \qquad \text{for all } t$$

$$\lim_{t \to \infty} K_1(t,1) = -\frac{1}{2} \quad ; \quad \lim_{t \to 0} K_1(t,1) = 0 \qquad\qquad \text{(A7)}$$

For $\eta < 1$, write Eq. (A3) as

$$K_2(t,\eta) = \{ t[(1-\eta)\cosh(1+\eta)t + (1+\eta)\cosh(1-\eta)t]$$

$$\div [\sinh(1+\eta)t + \sinh(1-\eta)t]\} / [4t + 2\sinh 2t] \qquad\qquad \text{(A8)}$$

To find the limits of K_1 and K_2 as t approaches zero and as t approaches infinity, use L'Hospital's rule to get

$$\lim_{|t| \to \infty} K_2(t,\eta) = 0 \qquad\qquad \text{for} \qquad \eta < 1$$

$$\lim_{|t| \to 0} K_1(t,\eta) = 0 \qquad\qquad \text{for} \qquad \eta \leq 1 \qquad\qquad \text{(A9)}$$

$$\lim_{|t| \to 0} K_2(t,\eta) = \frac{1}{2} \qquad\qquad \text{for} \qquad \eta \leq 1$$

With $t = \alpha + i\beta$, the limits of

$$K_1(t,\eta) e^{i\lambda t(1 \pm \psi)} \qquad \text{and} \qquad K_2(t,\eta) e^{i\lambda t(1 \pm \psi)} \quad ; \quad \lambda, \psi > 0$$

as t approaches zero and as t approaches infinity are

$$\lim_{\substack{|t| \to 0 \\ |t| \to \infty}} K_2(t,\eta) e^{i\lambda t(1 \pm \psi)} = \begin{cases} 0 \ \text{for} \quad \eta \leq 1 \ \text{as} \quad |t| \to \infty \ \begin{cases} \beta > 0 ; 1 \pm \psi \geq 0 \\ \beta < 0 ; 1 \pm \psi < 0 \end{cases} \\ 0 \ \text{for} \quad \eta \leq 1 \ \text{as} \quad |t| \to 0 \quad (\text{for } K_1) \\ \frac{1}{2} \ \text{for} \quad \eta \leq 1 \ \text{as} \quad |t| \to 0 \quad (\text{for } K_2) \end{cases} \qquad \text{(A10)}$$

Now the integrals in Eqs. (A1) and (A2) can be evaluated with the aid of the following integrals

$$\oint_{C_1} K_2(t, \eta) \, e^{i\lambda t(1 \pm \psi)} \, \frac{dt}{t} \qquad\qquad 1 \pm \psi \ge 0 \qquad\qquad \text{(A11)}$$

$$\oint_{C_2} K_2(t, \eta) \, e^{i\lambda t(1 - \psi)} \, \frac{dt}{t} \qquad\qquad \psi > 1 \qquad\qquad \text{(A12)}$$

where C_1 and C_2 are shown below
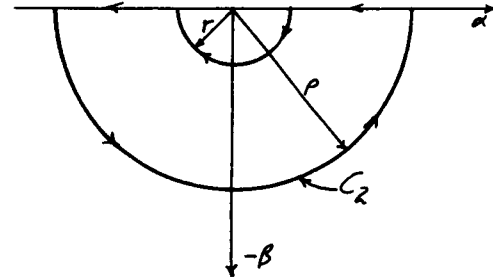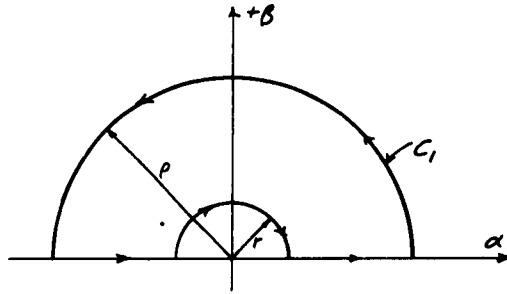
The typical integral in Eqs. (A11) and (A12) becomes

$$\oint_{C_1} K_1(t, \eta) \, e^{i\lambda t(1 \pm \psi)} \, \frac{dt}{t} = \int_{-\rho}^{-r} K_1(\alpha, \eta) \, e^{i\lambda\alpha(1 \pm \psi)} \, \frac{d\alpha}{\alpha}$$

$$+ i \int_{\pi}^{0} K_1(t_r, \eta) \, e^{i\lambda t_r(1 \pm \psi)} \, d\theta$$

$$+ \int_{r}^{\rho} K_1(\alpha, \eta) \, e^{i\lambda\alpha(1 \pm \psi)} \, \frac{d\alpha}{\alpha}$$

$$+ i \int_{0}^{\pi} K_1(t_\rho, \eta) \, e^{i\lambda t_\rho(1 \pm \psi)} \, d\theta$$

22

or

$$\oint_{C_1} K_1(t,\eta) e^{i\lambda t(1\pm\psi)} \frac{dt}{t} = 2i \int_r^{\rho} K_1(a,\eta) SIN \lambda a(1\pm\psi) \frac{da}{a}$$

$$+ i \int_{\pi}^{0} K_1(t_r,\eta) e^{i\lambda t_r(1\pm\psi)} d\theta$$

$$+ i \int_0^{\pi} K_1(t_\rho,\eta) e^{i\lambda t_\rho(1\pm\psi)} d\theta$$

$$= 2\pi i \sum \text{Residues at poles in } C_1 \qquad (A13)$$

In the limit as ρ approaches infinity and r approaches zero, Eq. (A13) gives

$$\int_0^{\infty} K_1(a,\eta) SIN \lambda a(1\pm\psi) \frac{da}{a} = \pi \sum \text{Residues at poles in the upper half plane}$$

$$= \left\{ \begin{array}{c} \pi R_1 \\ \pi R_3 \end{array} \right\} \quad \text{for} \quad 1\pm\psi \geq 0 \qquad (A14)$$

where the integrals around the semi-circles are zero in the limit by Eq. (A10). By using Eq.(10a) and the procedure of Eq. (A13), the other integrals in Eqs. (A11) and (A12) give

$$\left. \begin{array}{l} \displaystyle\int_0^{\infty} K_2(a,\eta) SIN \lambda a(1\pm\psi) \frac{da}{a} = \frac{\pi}{4} + \left\{ \begin{array}{c} \pi R_2 \\ \pi R_4 \end{array} \right\} \quad \text{for} \quad 1\pm\psi>0 \\[4em] \displaystyle\int_0^{\infty} K_2(a,\eta) SIN \lambda a(1-\psi) \frac{da}{a} = \left\{ \begin{array}{c} -\pi R_5 \\ -\frac{\pi}{4} - \pi R_6 \end{array} \right\} \quad \text{for} \quad \psi>1 \end{array} \right\} \qquad (A15)$$

$$\int_0^{\infty} K_1(t,\eta) SIN \lambda t COS \lambda \psi t \frac{dt}{t} = \left\{ \begin{array}{ll} \frac{\pi}{2}[R_1+R_3] & \text{for} \quad |\psi|<1 \\ \frac{\pi}{2} R_1 & \text{for} \quad |\psi|=1 \\ \frac{\pi}{2}[R_1-R_5] & \text{for} \quad |\psi|>1 \end{array} \right. \qquad (A16)$$

23

$$\int_0^\infty [K_2(t,\eta) - \tfrac{1}{2}] \, SIN\lambda t \, COS\lambda \eta t \, \frac{dt}{t} = \begin{cases} \frac{\pi}{2}[R_2 + R_4] & \text{for} & |\eta| < 1 \\ \frac{\pi}{2}R_2 & \text{for} & |\eta| = 1 \\ \frac{\pi}{2}[R_2 - R_6] & \text{for} & |\eta| > 1 \end{cases} \qquad (A17)$$

The poles of $K_1(t,\eta)$ and $K_2(t,\eta)$ are given by the non-zero t_n such that

$$SINH2t_n + 2t_n = 0$$

or

$$SINH2\alpha_n \, COS2\beta_n + 2\alpha_n = 0 \qquad (A18)$$

$$COSH2\alpha_n \, SIN2\beta_n + 2\beta_n = 0 \qquad (A19)$$

From Eq. (A18)

$$COS2\beta_n = -2\alpha_n / SINH2\alpha_n \qquad (A20)$$

so that

$$2\beta_n = ARCCOS[-2\alpha_n / SINH2\alpha_n] \qquad (A21)$$

$$SIN2\beta_n = \pm[1 - (2\alpha_n/SINH2\alpha_n)^2]^{\frac{1}{2}} \qquad (A22)$$

Substituting Eqs. (A21) and (A22) into Eq. (A19), there results

$$COS\{[COSH2\alpha_n][1 - (2\alpha_n/SINH2\alpha_n)^2]^{\frac{1}{2}}\} = 2\alpha_n / SINH2\alpha_n \qquad (A23)$$

24

Therefore if α_n is a root of Eq. (A23), $-\alpha_n$ is also a root; if β_n corresponds to the root α_n through Eq. (A21), then $-\beta_n$ also corresponds to α_n and $\pm \beta_n$ corresponds to $-\alpha_n$. Thus if $t_n = \alpha_n \pm i\beta_n$ is a root of Eqs. (A18) and (A19), then $\bar{t}_n = \alpha_n - i\beta_n$, $-t_n = -\alpha_n - i\beta_n$, and $-\bar{t}_n = -\alpha_n + i\beta_n$ are also roots. From Eq. (A23), as α_n becomes large

$$COSH\, 2\alpha_n \approx \frac{2m+1}{2}\,\pi$$

or

$$\alpha_n \approx \frac{1}{2}\,ln\,[\pi(2m+1)]$$

and from Eq. (A24)

$$\beta_n \approx \frac{1}{4}\,(2m+1)\,\pi$$

Hence for large n, the poles are given approximately by

$$t_n = \pm \frac{1}{2}\,ln\,[\pi(2m+1)] \pm i\,\frac{\pi}{4}(2m+1)$$

Seewald (Ref. 17) lists the first four positive roots of Eq. (A23) as

$$
\begin{aligned}
\alpha_1 &= 1.1415 \,; & \beta_1 &= 2.1142 \\
\alpha_2 &= 1.533 \,; & \beta_2 &= 5.359 \\
\alpha_3 &= 1.766 \,; & \beta_3 &= 8.537 \\
\alpha_4 &= 1.925 \,; & \beta_4 &= 11.70
\end{aligned}
$$

The residue of the integrands at the pole t_n is given by γ_n where

$$\gamma_{in}^{\pm} = \lim_{t \to t_n}\ K_i(t,\eta)\,e^{i\lambda t(1\pm\mu)}\left[\frac{t - t_n}{t}\right]$$

25

or

$$Y_{2m}^{\pm} = \lim_{t \to t_m} \frac{(t - t_m) N_{\frac{1}{2}}(t, \gamma) e^{i\lambda t (1 \pm \gamma)}}{\lambda (SINH2t + 2t)}$$

or

$$Y_{2m}^{\pm} = \frac{N_{\frac{1}{2}}(t_m, \gamma) e^{i\lambda t_m (1 \pm \gamma)}}{2 t_m (COSH2t_m + 1)}$$

Now let

$$2 t_m (COSH2t_m + 1) = C_m + i D_m = \bar{C}_m e^{i \bar{D}_m}$$

and

$$N_{\frac{1}{2}}(t_m, \gamma) = A_{2m} + i B_{2m} = \bar{A}_{2m} e^{i \bar{B}_{2m}}$$

then

$$Y_{2m}^{\pm} = [1/\bar{C}_m^2][e^{-\lambda B_m (1 \pm \gamma)}]\![(A_{2m} C_m + B_{2m} D_m)(COS \lambda d_m (1 \pm \gamma)$$

$$+ i SIN \lambda d_m (1 \pm \gamma)]$$

$$- (B_{2m} C_m - A_{2m} D_m)(SIN \lambda d_m (1 \pm \gamma)$$

$$- i COS \lambda d_m (1 \pm \gamma))]$$

26

Therefore

$$R_1 = \sum_{n=1}^{\infty} \left[Y_{1n}^+(t_n) + Y_{1n}^\tau(-\bar{t}_n) \right]$$

or

$$R_1 = \sum_{n=1}^{\infty} \left\{ [2/\bar{C}_n^2][(A_{1n}C_n + B_{1n}D_n)\cos\lambda d_n(1+\psi) \right.$$
$$\left. - (B_{1n}C_n - A_{1n}D_n)\sin\lambda d_n(1+\psi)] e^{-\lambda B_n(1+\psi)} \right\}$$

and similarly

$$R_2 = \sum_{n=1}^{\infty} \left\{ [2/\bar{C}_n^2][(A_{2n}C_n + B_{2n}D_n)\cos\lambda d_n(1+\psi) \right.$$
$$\left. - (B_{2n}C_n - A_{2n}D_n)\sin\lambda d_n(1+\psi)] e^{-\lambda B_n(1+\psi)} \right\}$$

$$R_3 = \sum_{n=1}^{\infty} \left\{ [2/\bar{C}_n^2][(A_{1n}C_n + B_{1n}D_n)\cos\lambda d_n(1-\psi) \right.$$
$$\left. - (B_{1n}C_n - A_{1n}D_n)\sin\lambda d_n(1-\psi)] e^{-\lambda B_n(1-\psi)} \right\}$$

$$R_4 = \sum_{n=1}^{\infty} \left\{ [2/\bar{C}_n^2][(A_{2n}C_n + B_{2n}D_n)\cos\lambda d_n(1-\psi) \right.$$
$$\left. - (B_{2n}C_n - A_{2n}D_n)\sin\lambda d_n(1-\psi)] e^{-\lambda B_n(1-\psi)} \right\}$$

$$R_5 = \sum_{n=1}^{\infty} \left\{ [2/\bar{C}_n^2][(A_{1n}C_n + B_{1n}D_n)\cos\lambda d_n(1-\psi) \right.$$
$$\left. + (B_{1n}C_n - A_{1n}D_n)\sin\lambda d_n(1-\psi)] e^{\lambda B_n(1-\psi)} \right\}$$

$$R_6 = \sum_{n=1}^{\infty} \left\{ [2/\bar{C}_n^2][(A_{2n}C_n + B_{2n}D_n)\cos\lambda d_n(1-\psi) \right.$$
$$\left. + (B_{2n}C_n - A_{2n}D_n)\sin\lambda d_n(1-\psi)] e^{\lambda B_n(1-\psi)} \right\}$$

(A24)

Finally from Eqs. (A16), (A17), and (A24), the integrals of Eqs. (A1) and (A2) can be expressed

$$\int_0^\infty K_1(t,\gamma)\,SIN\,\lambda t\,COS\,\lambda \gamma t\,\frac{dt}{t} = \pi \sum_{n=1}^\infty [f_{1m}(\gamma)\,G_{1n}(\lambda,\gamma) - f_{2m}(\gamma)\,G_{2n}(\lambda,\gamma)]$$

$$\int_0^\infty [K_2(t,\gamma) - \tfrac{1}{2}]\,SIN\,\lambda t\,COS\,\lambda \gamma t\,\frac{dt}{t} = \pi \sum_{n=1}^\infty [f_{3m}(\gamma)\,G_{1m}(\lambda,\gamma) - f_{4m}(\gamma)\,G_{2m}(\lambda,\gamma)]$$

where

$$f_{1m}(\gamma) = (A_{1m}C_n + B_{1m}D_n)/\bar{C}_n^2 \quad ; \quad f_{2m}(\gamma) = (B_{1m}C_n - A_{1m}D_n)/\bar{C}_n^2$$

$$f_{3m}(\gamma) = (A_{2n}C_n + B_{2m}D_n)/\bar{C}_n^2 \quad ; \quad f_{4m}(\gamma) = (B_{2n}C_n - A_{2n}D_n)/\bar{C}_n^2$$

$$G_{1n}(\lambda,\gamma) = \begin{cases} e^{-\lambda\beta_n(1+\gamma)}COS\,\lambda d_m(1+\gamma) \\ \qquad + e^{-\lambda\beta_n(1-\gamma)}COS\,\lambda d_n(1-\gamma) & ; \; 0 \le \gamma < 1 \\[2ex] e^{-\lambda\beta_n(1+\gamma)}COS\,\lambda d_m(1+\gamma) & ; \; \gamma = 1 \\[2ex] e^{-\lambda\beta_n(1+\gamma)}COS\,\lambda d_n(1+\gamma) \\ \qquad - e^{\lambda\beta_n(1-\gamma)}COS\,\lambda d_n(1-\gamma) & ; \; \gamma > 1 \end{cases}$$

$$G_{2m}(\lambda,\gamma) = \begin{cases} e^{-\lambda\beta_n(1+\gamma)}SIN\,\lambda d_n(1+\gamma) \\ \qquad + e^{-\lambda\beta_n(1-\gamma)}SIN\,\lambda d_n(1-\gamma) & ; \; 0 \le \gamma < 1 \\[2ex] e^{-\lambda\beta_n(1+\gamma)}SIN\,\lambda d_m(1+\gamma) & ; \; \gamma = 1 \\[2ex] e^{-\lambda\beta_n(1+\gamma)}SIN\,\lambda d_m(1+\gamma) \\ \qquad + e^{\lambda\beta_n(1-\gamma)}SIN\,\lambda d_n(1-\gamma) & ; \; \gamma > 1 \end{cases}$$

28

where

$$A_{2m} = \frac{1}{2}\{R_m(1-\eta)[COSH\alpha_m(1+\eta)COS\beta_m(1+\eta)COS\theta_m$$

$$- SINH\alpha_m(1+\eta)SIN\beta_m(1+\eta)SIN\theta_m]$$

$$+ R_m(1+\eta)[COSH\alpha_m(1-\eta)COS\beta_m(1-\eta)COS\theta_m$$

$$- SINH\alpha_m(1-\eta)SIN\beta_m(1-\eta)SIN\theta_m]$$

$$\mp SINH\alpha_m(1+\eta)COS\beta_m(1+\eta)$$

$$\mp SINH\alpha_m(1-\eta)COS\beta_m(1-\eta)\}$$

$$B_{2m} = \frac{1}{2}\{R_m(1-\eta)[COSH\alpha_m(1+\eta)COS\beta_m(1+\eta)SIN\theta_m$$

$$+ SINH\alpha_m(1+\eta)SIN\beta_m(1+\eta)COS\theta_m]$$

$$+ R_m(1+\eta)[COSH\alpha_m(1-\eta)COS\beta_m(1-\eta)SIN\theta_m$$

$$+ SINH\alpha_m(1-\eta)SIN\beta_m(1-\eta)COS\theta_m]$$

$$\mp COSH\alpha_m(1+\eta)SIN\beta_m(1+\eta)$$

$$\mp COSH\alpha_m(1-\eta)SIN\beta_m(1-\eta)\}$$

$$C_m = 2[\alpha_m(COSH2\alpha_m COS2\beta_m +1) - \beta_m SINH2\alpha_m SIN2\beta_m]$$

$$D_m = 2[\beta_m(COSH2\alpha_m COS2\beta_m +1) + \alpha_m SINH2\alpha_m SIN2\beta_m]$$

with

$$R_m^2 = \alpha_m^2 + \beta_m^2 \ ; \quad \bar{C}_m^2 = C_m^2 + D_m^2 \ ; \quad COS\theta_m = \frac{\alpha_m}{R_m} \ ; \quad SIN\theta_m = \frac{\beta_m}{R_m}$$

Figure 2: Comparison of Przemieniecki's and Timoshenko's Solution for $T = -T_0 \cos(\frac{4\pi y}{L})$ at $(X/L) = 0.75$
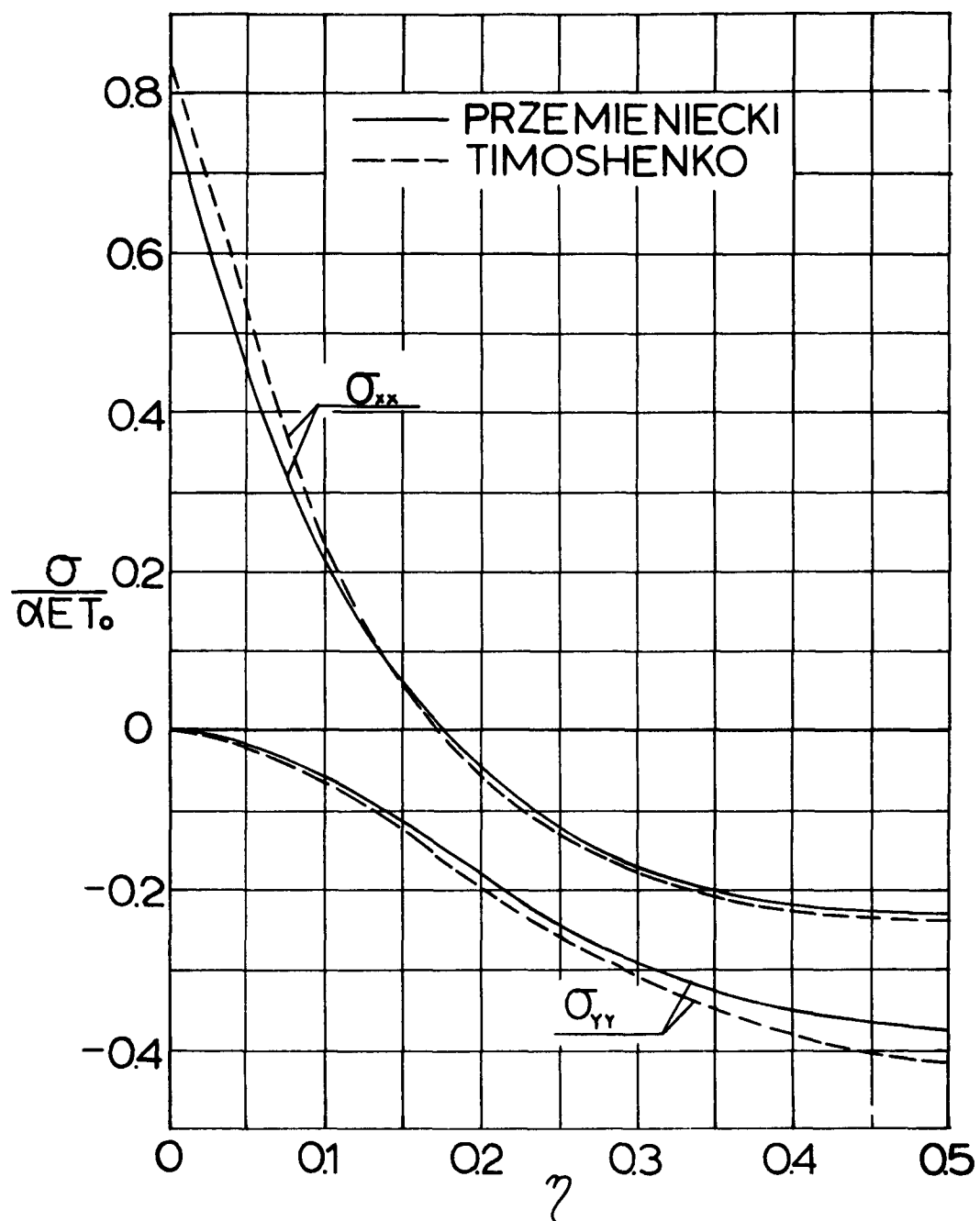
Figure 3: Comparison of Przemieniecki's and
Timoshenko's Solution for $T=-T_0 COS(4\pi x/L)$
at $(X/L) = 0.25$

31
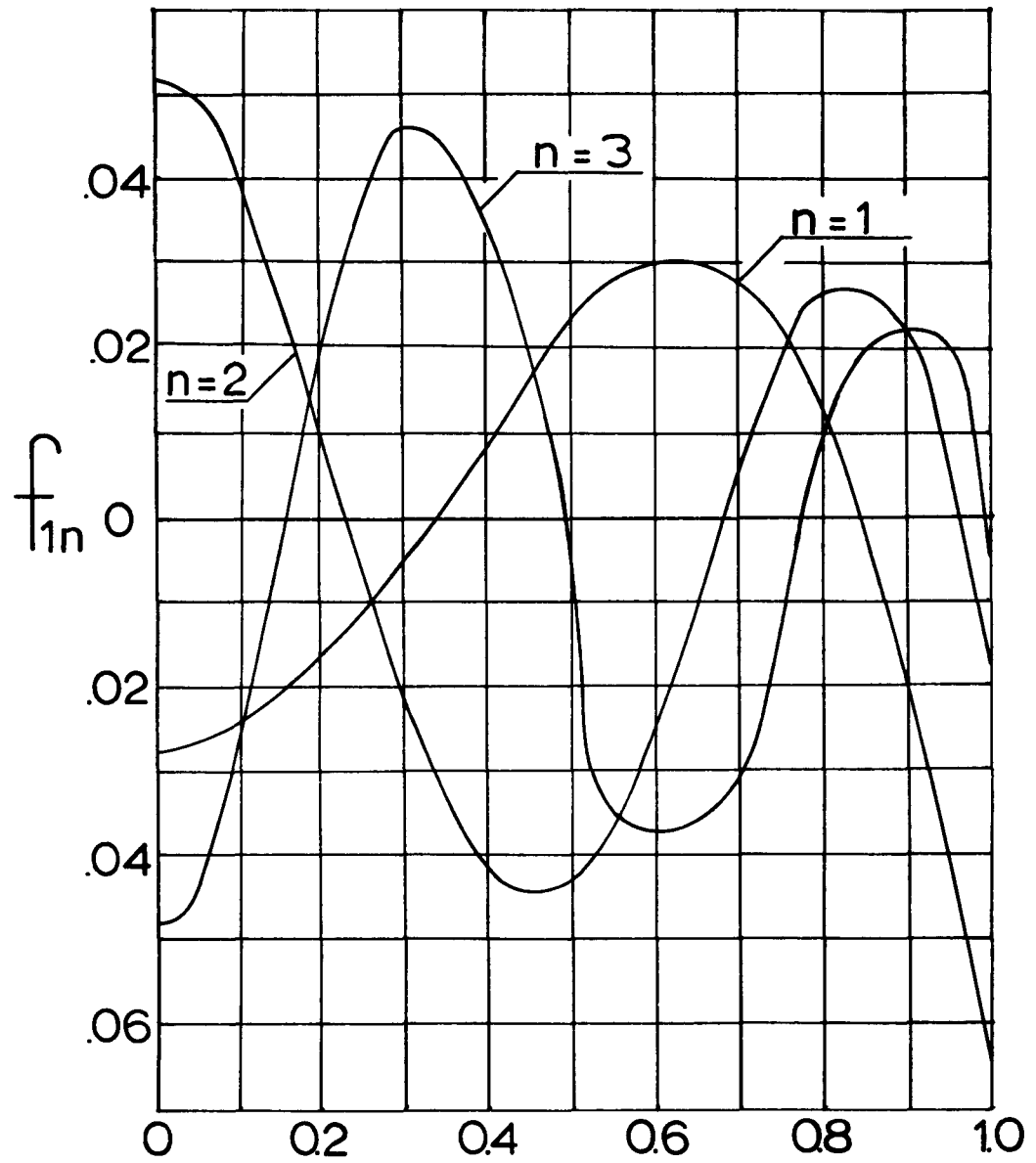
Figure 5: Graph of $f_{1n}(\eta)$ vs η for $n = 1,2,3$

32
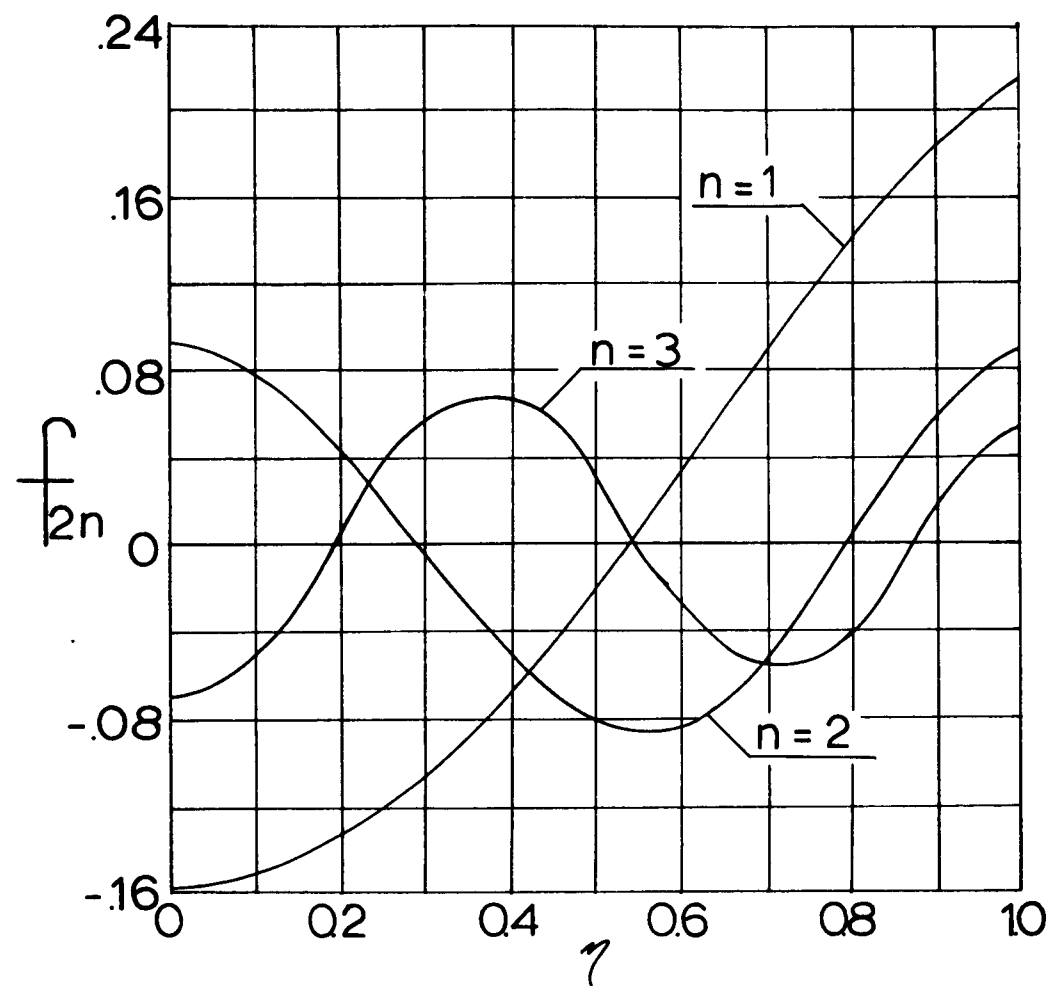
Figure 6: Graph of $f_{2n}(\eta)$ vs η for $n = 1,2,3$

33
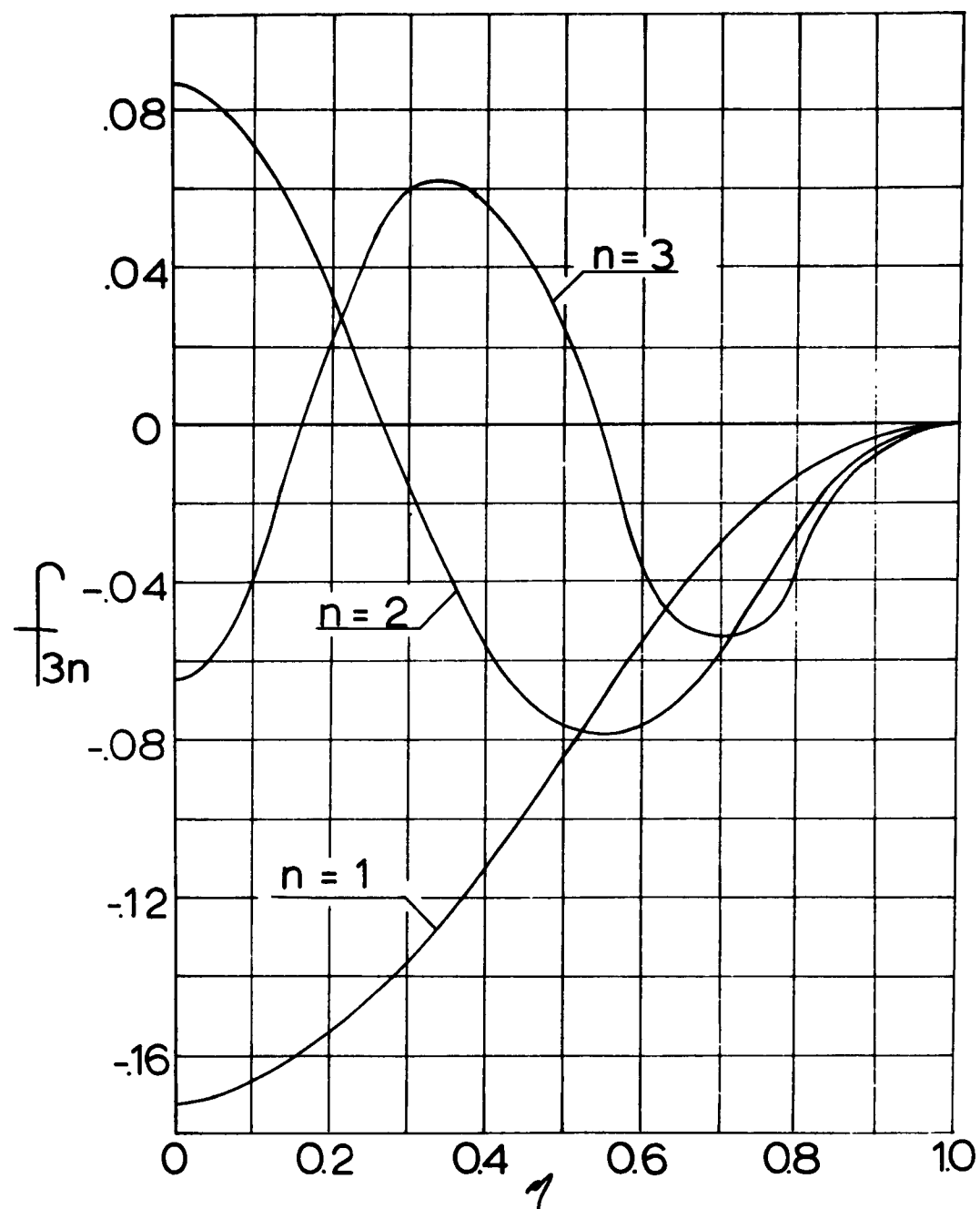
Figure 7: Graph of $f_{3n}(\eta)$ vs η for $n = 1,2,3$

34
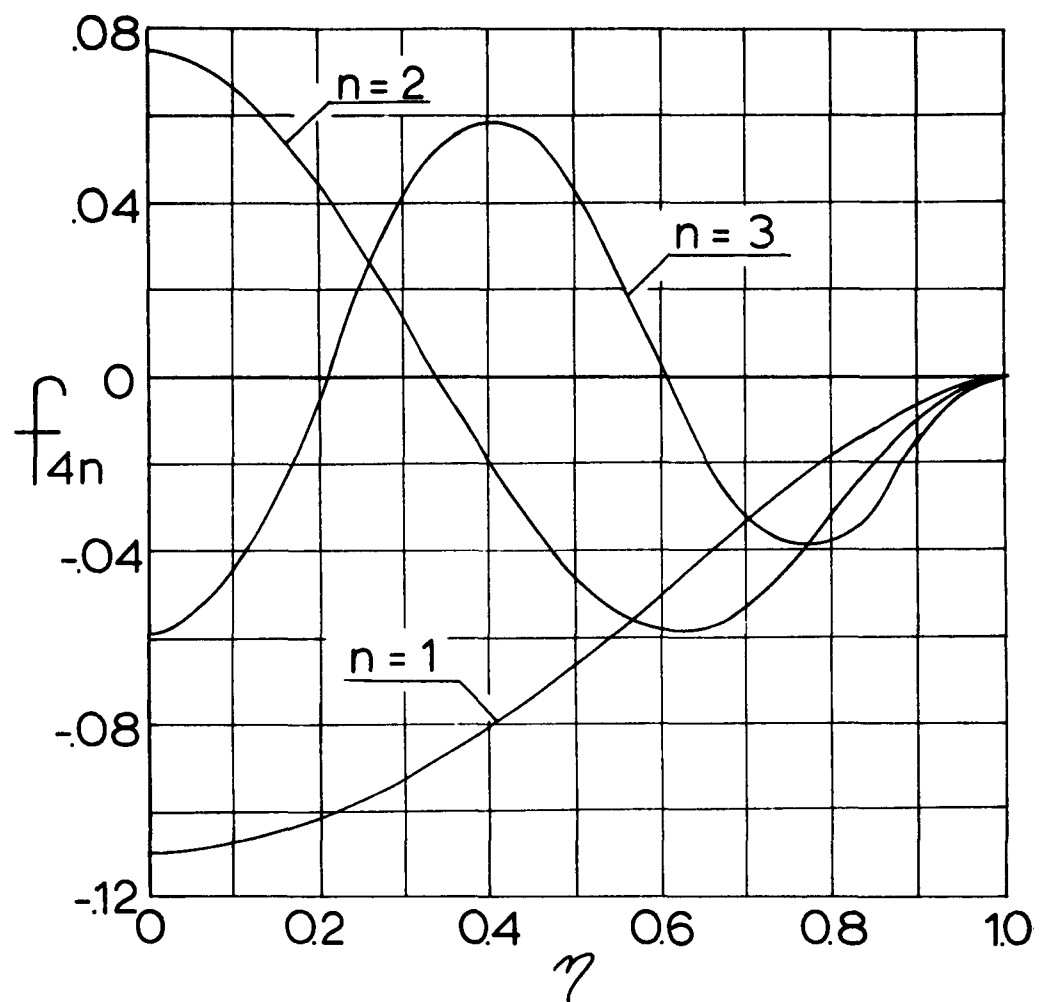
Figure 8: Graph of $f_{4n}(\eta)$ vs η for $n = 1,2,3$

35
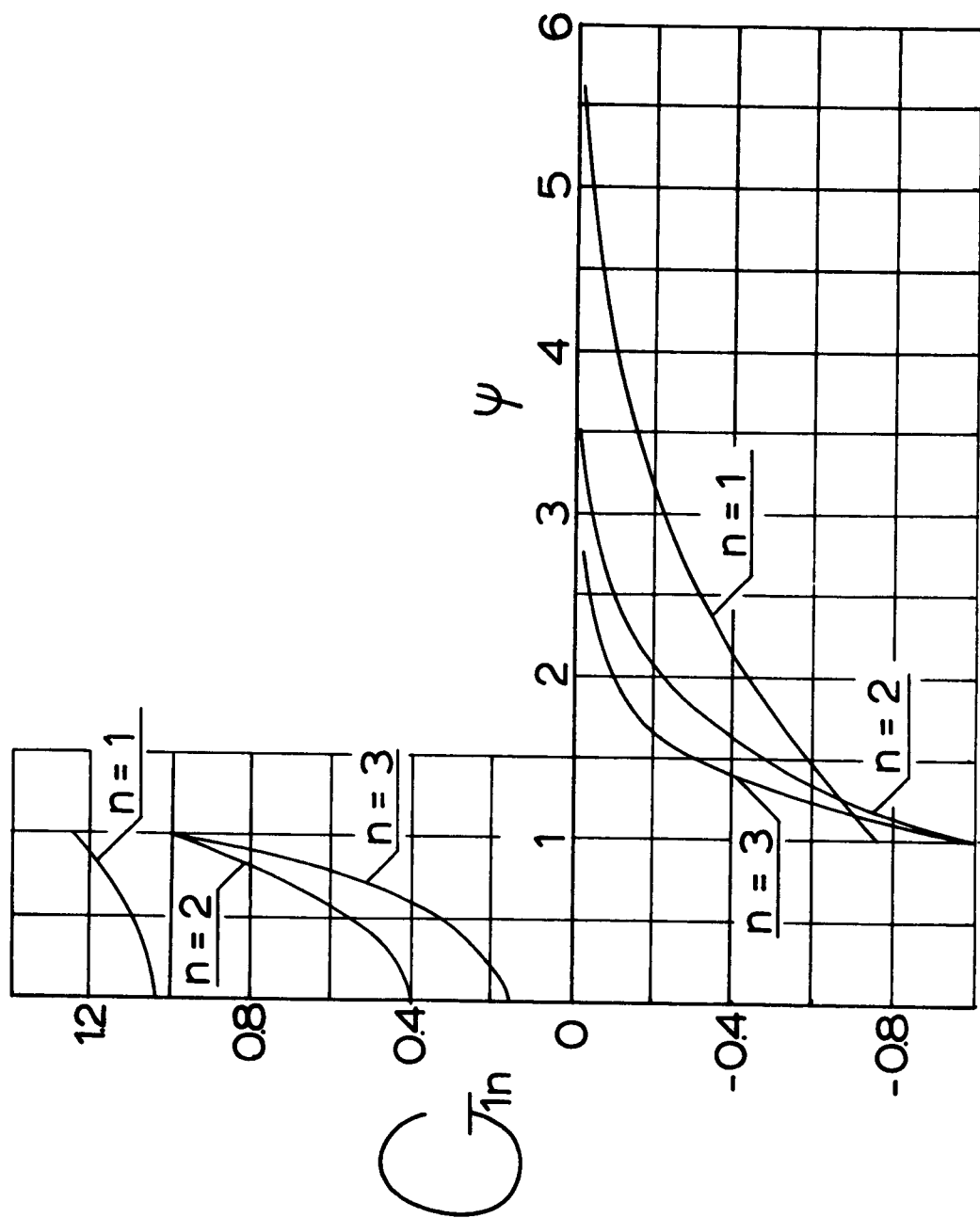
Figure 9: Graph of $G_{1n}(\lambda,\psi)$ vs ψ for $\lambda = 0.27775$ and $n = 1,2,3$

36
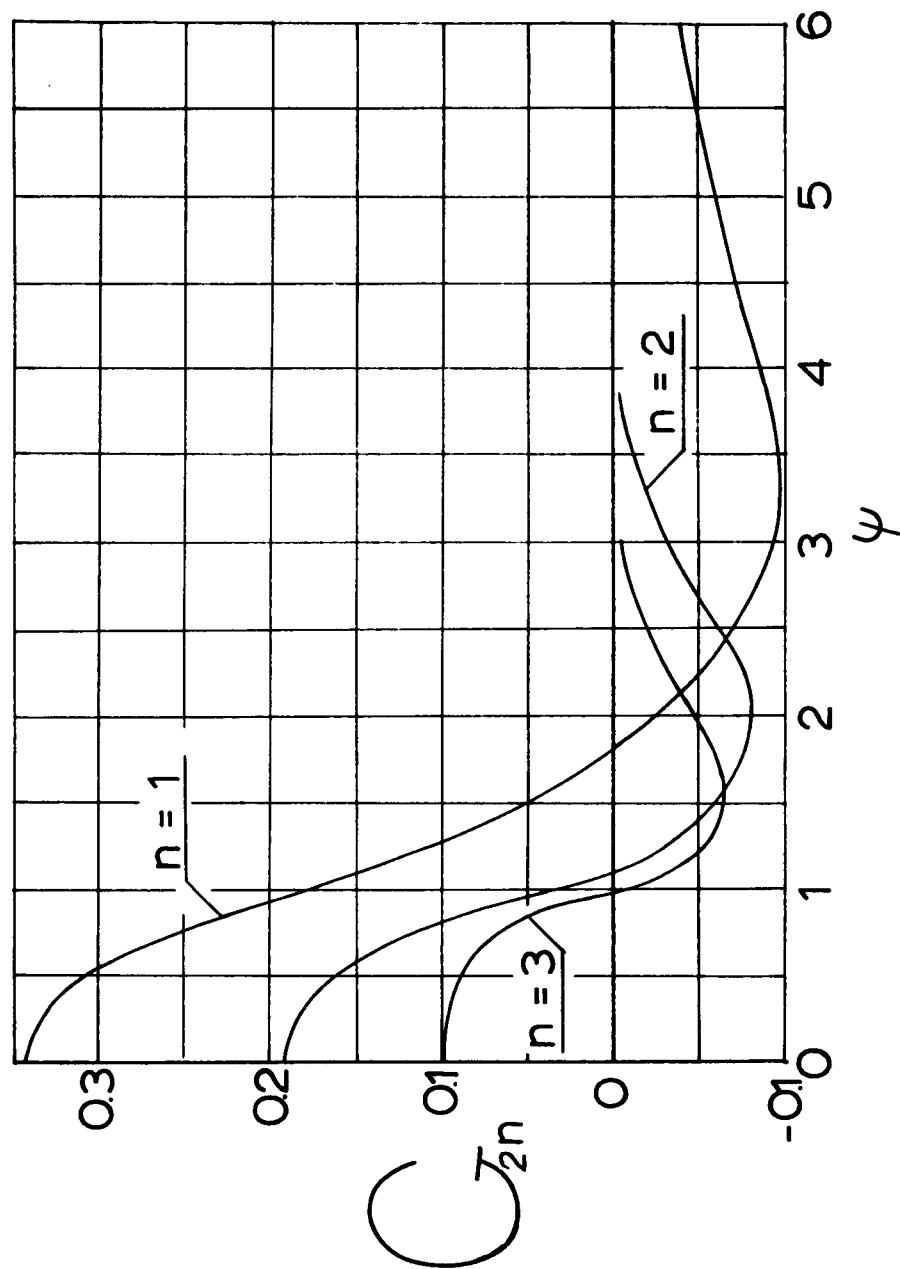
Figure 10: Graph of $G_{2n}(\lambda, \psi)$ vs ψ for $\lambda = 0.27775$ and $n = 1, 2, 3$

A: Cooling Tube Used
     With Four Wave Case
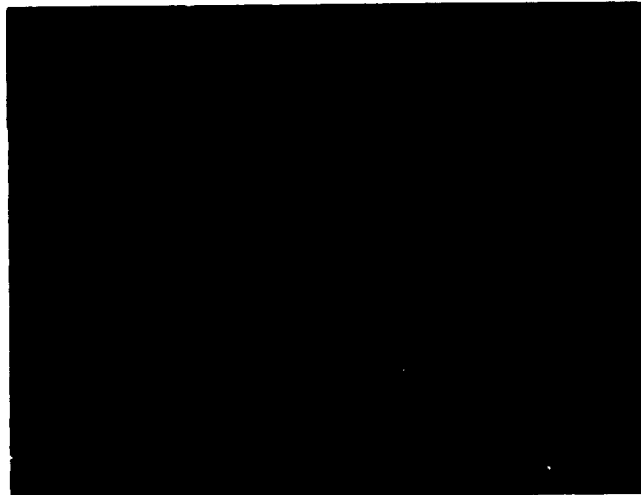
B: Cooling Tube Used
     With Short Wave Case

Figure 11:   Photographs of Cooling Tubes
             Used to Provide Heat Sinks
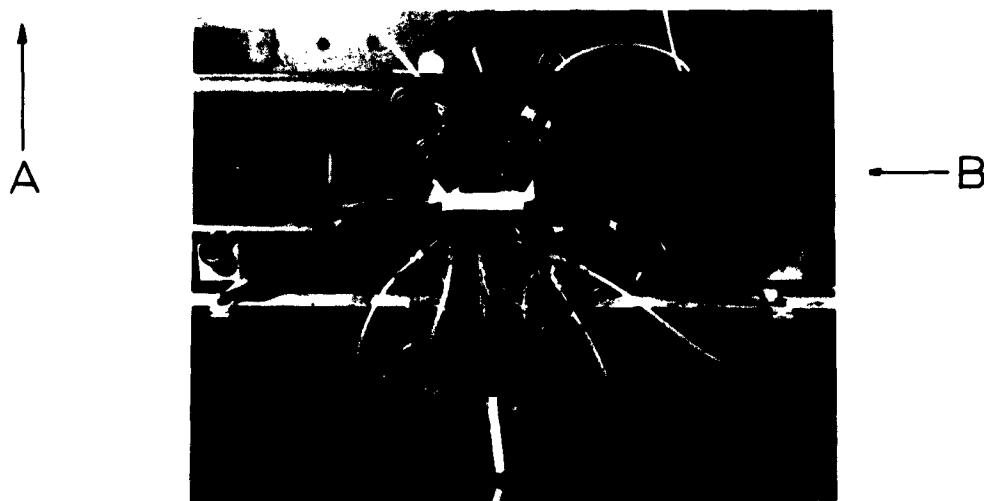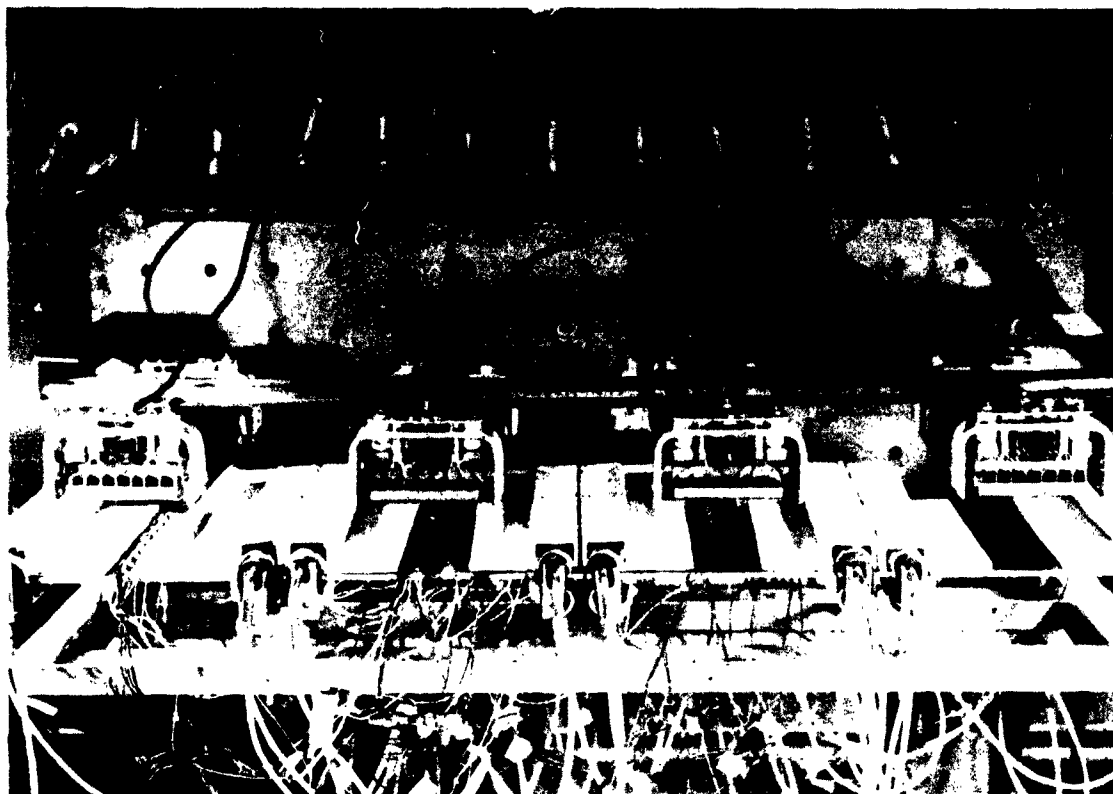
Figure 12: Configurations Used to Produce
Desired Temperature Distributions
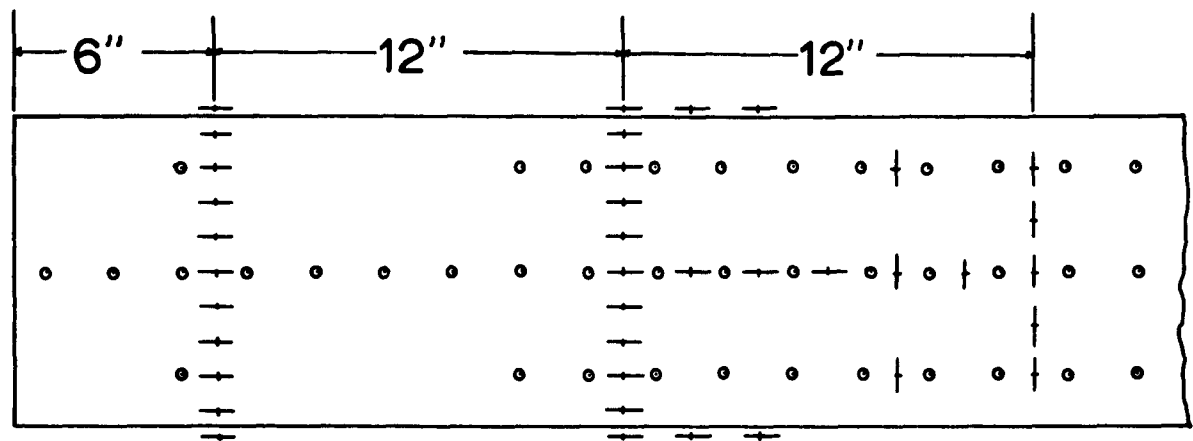
A: FOUR WAVE CASE

⊙ thermocouples

+ ⊷ strain gages
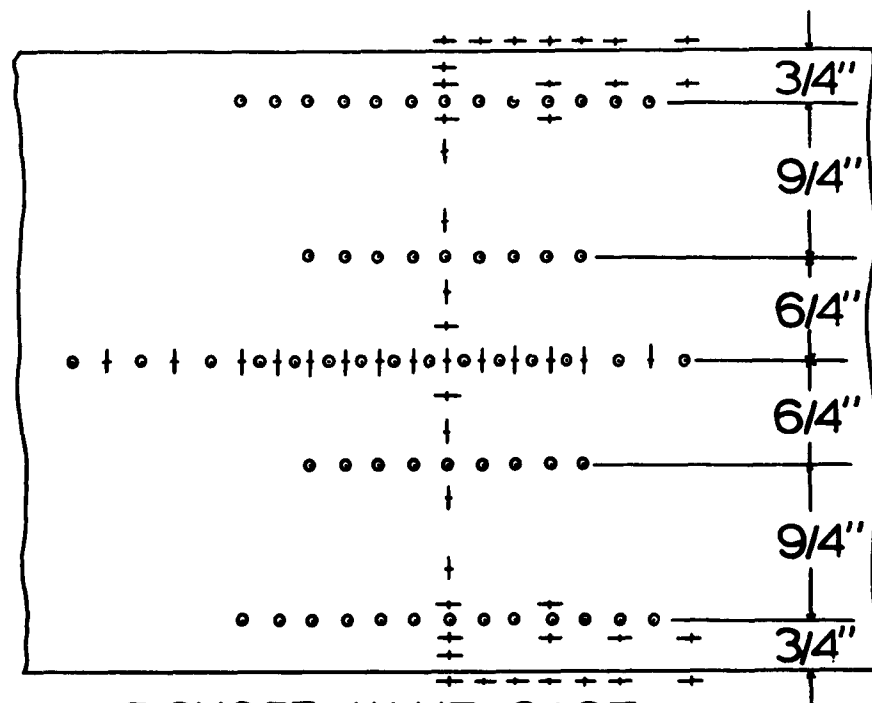
B: SHORT WAVE CASE

Figure 13: Location of Thermocouples and Strain Gages on Test Specimen
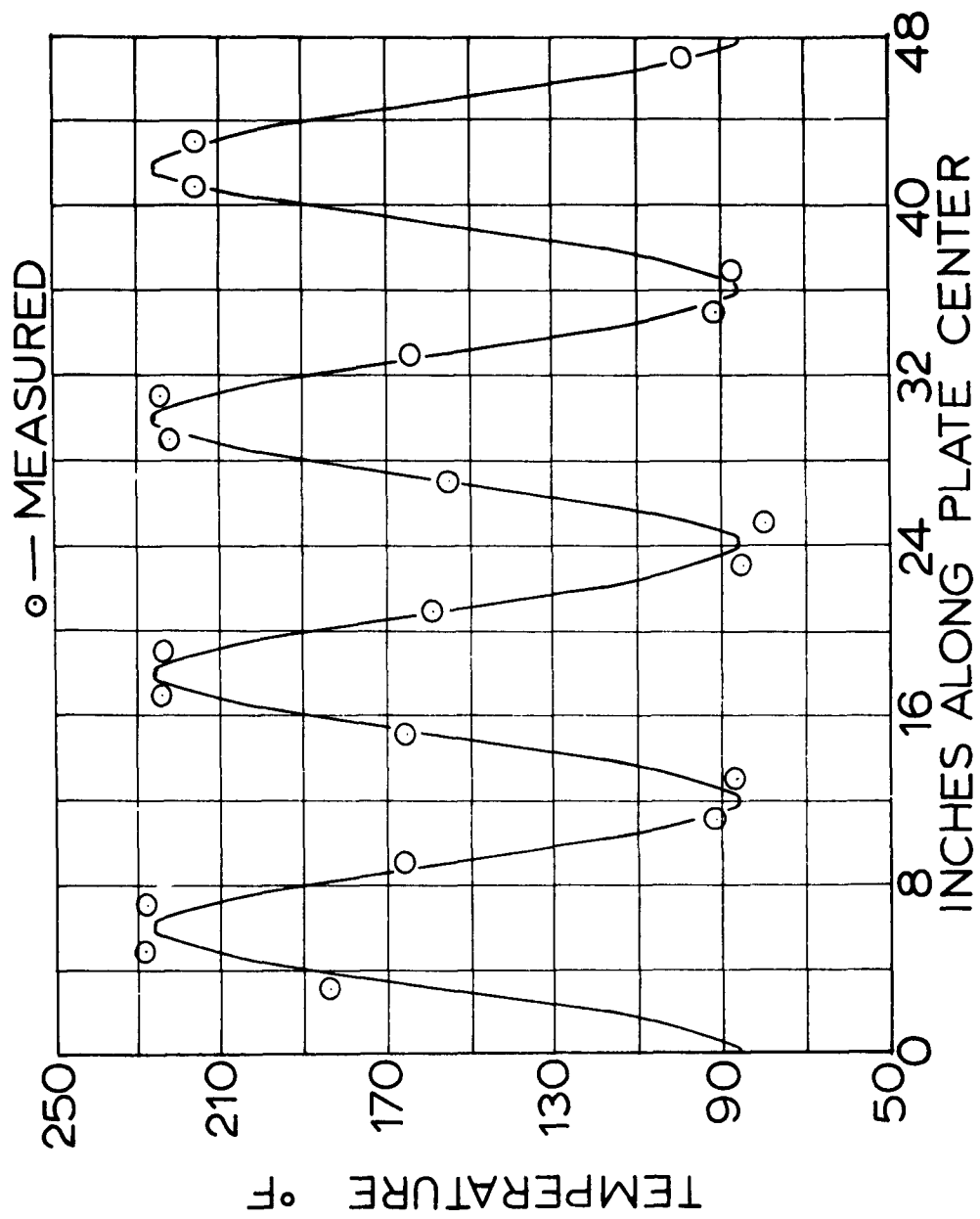
Figure 14: Comparison of Measured Temperature with
Cosinusodial Distribution; Test 1

41
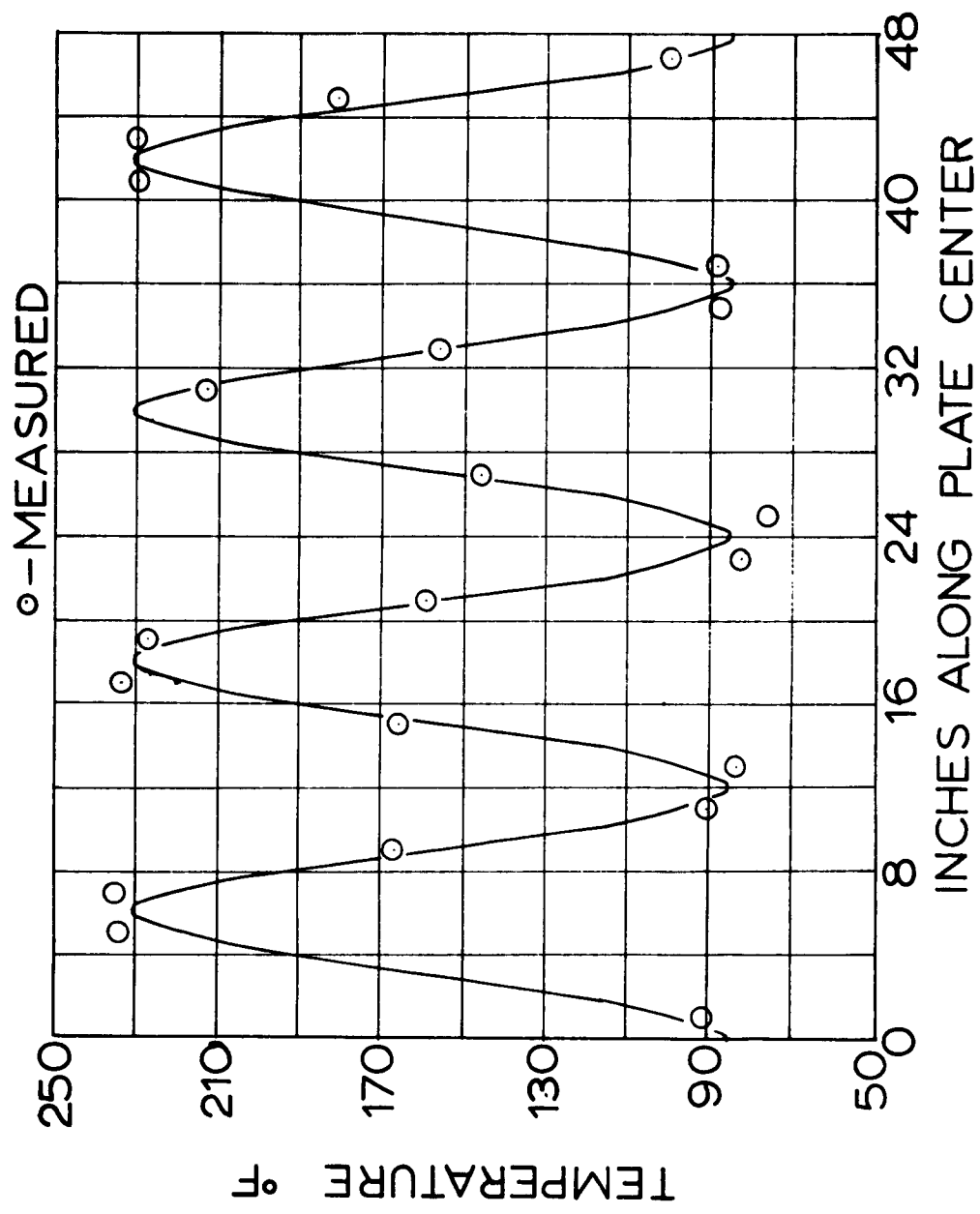
Figure 15: Comparison of Measured Temperature with
Cosinusodial Distribution; Test 2
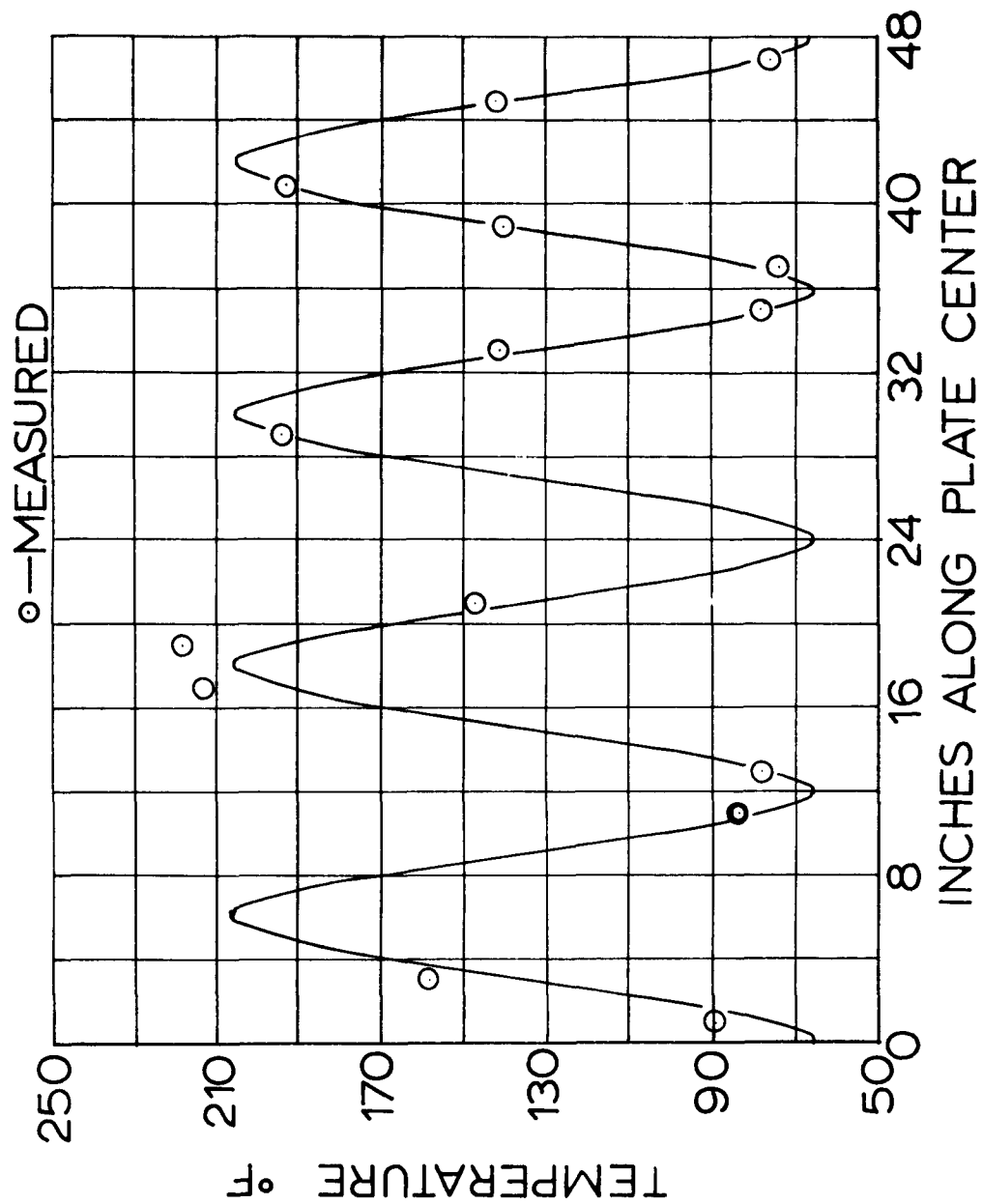
Figure 16: Comparison of Measured Temperature with Cosinusodial Distribution; Test 3
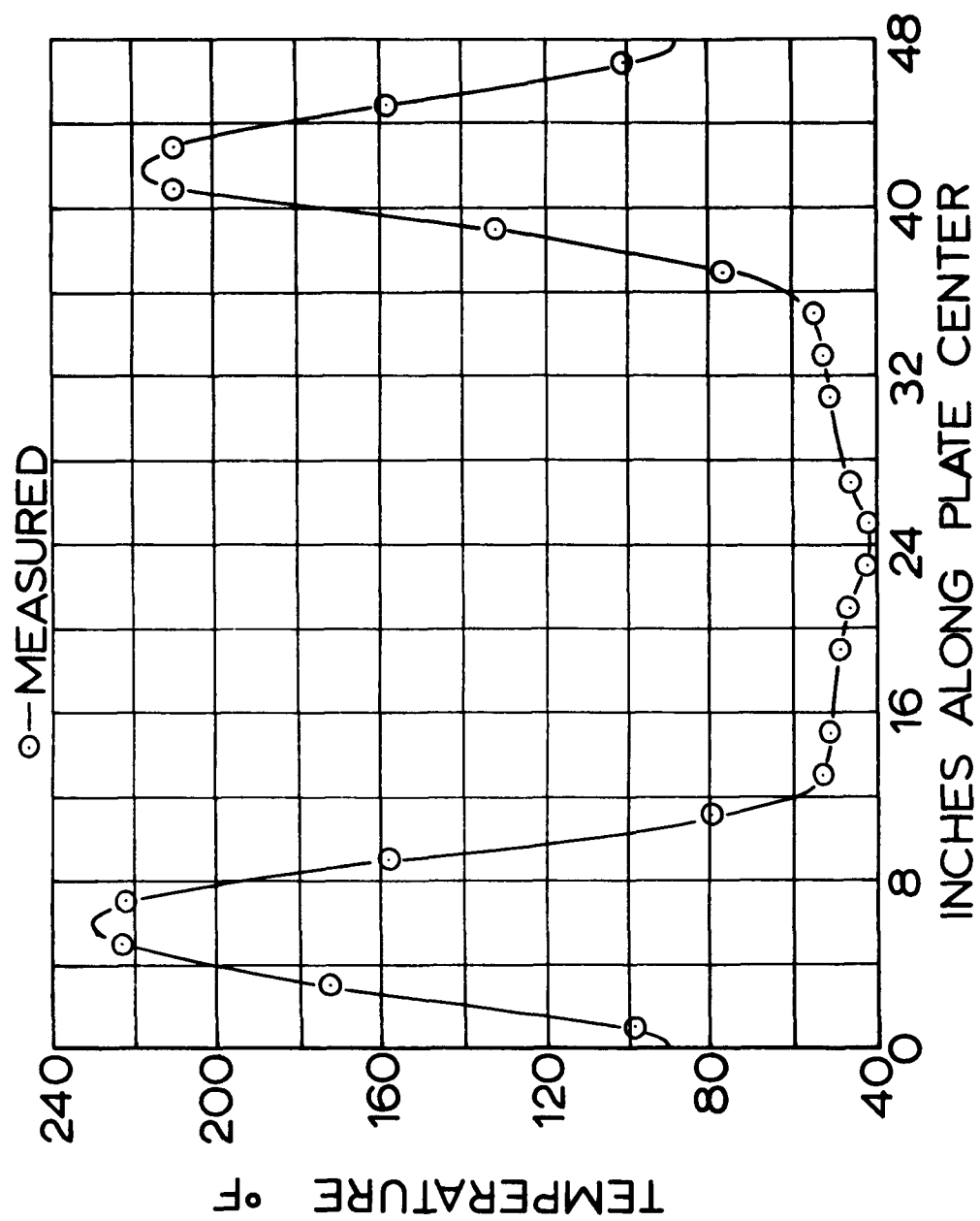
Figure 17: Measured Temperature Distribution; Test 4

44
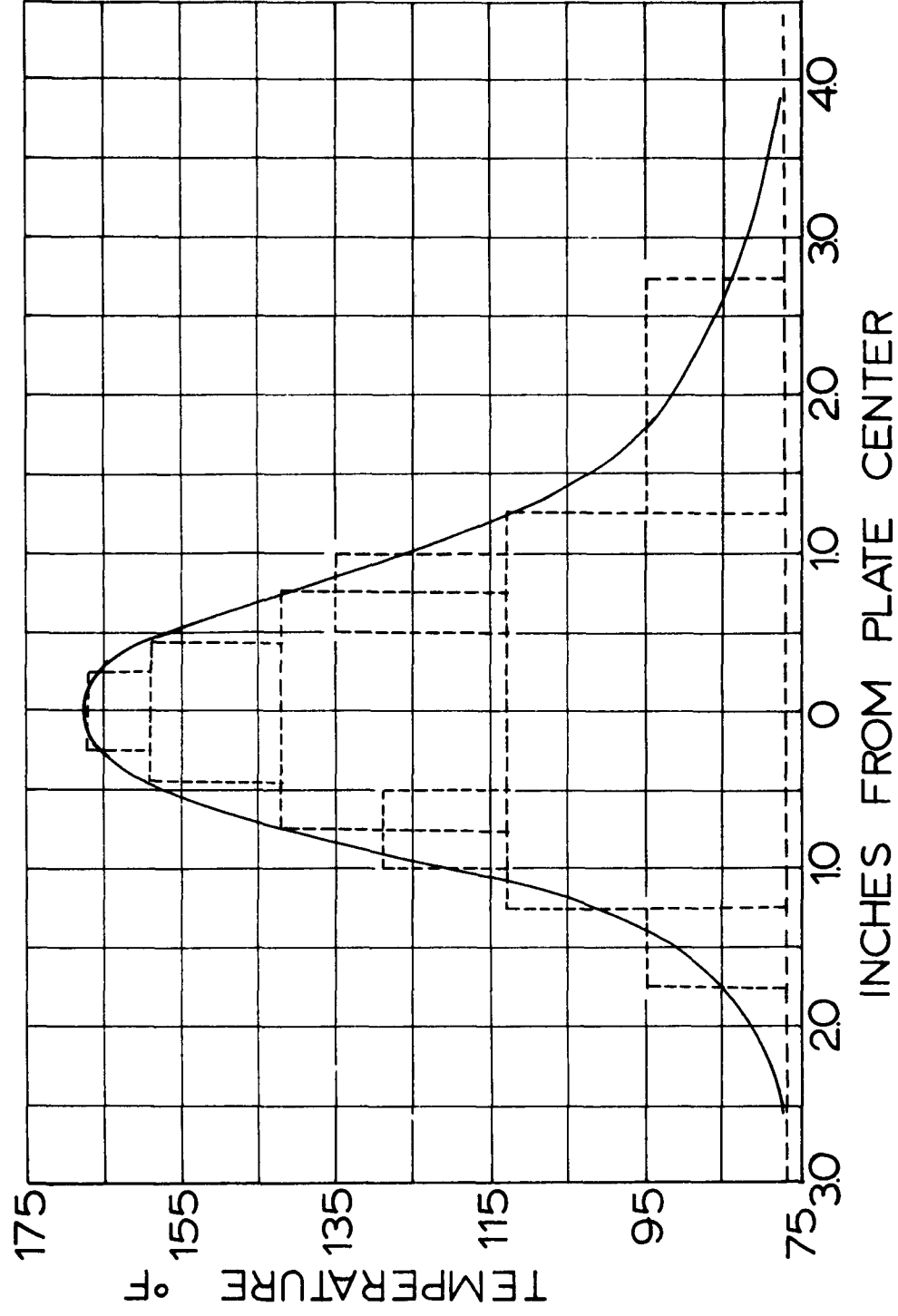
Figure 18:   Average Spanwise Temperature
Distribution Obtained for Short
Wave Case with Approximating
Temperature Steps
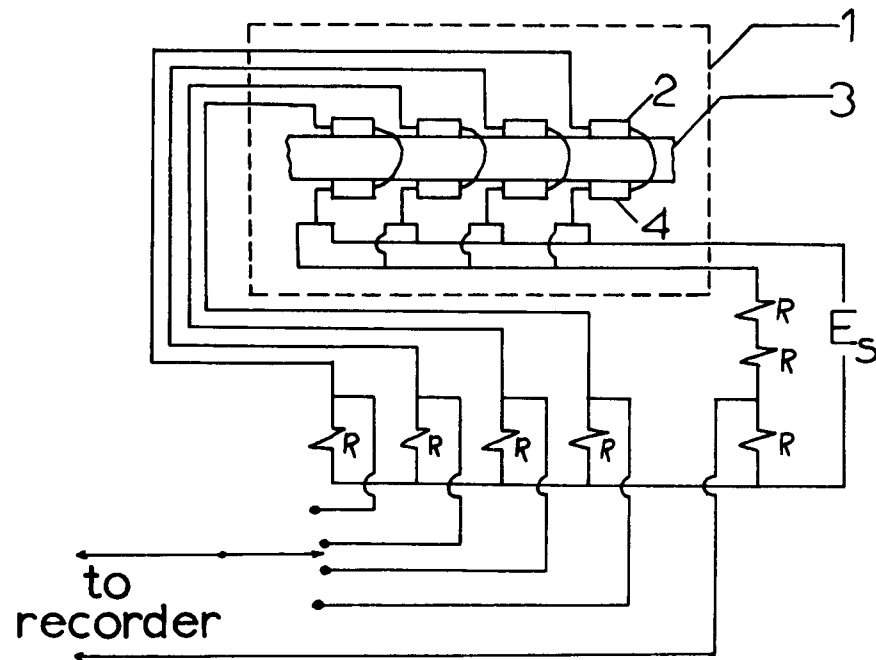
1: all connections within dotted lines made near specimen

2: strain gage on upper surface

3: specimen

4: strain gage on lower surface

R: 120Ω precision resistors

E_s: D.C. supply voltage

Figure 19: Electrical Circuit Used with Four Wave Case Employing a Three-Wire Lead System
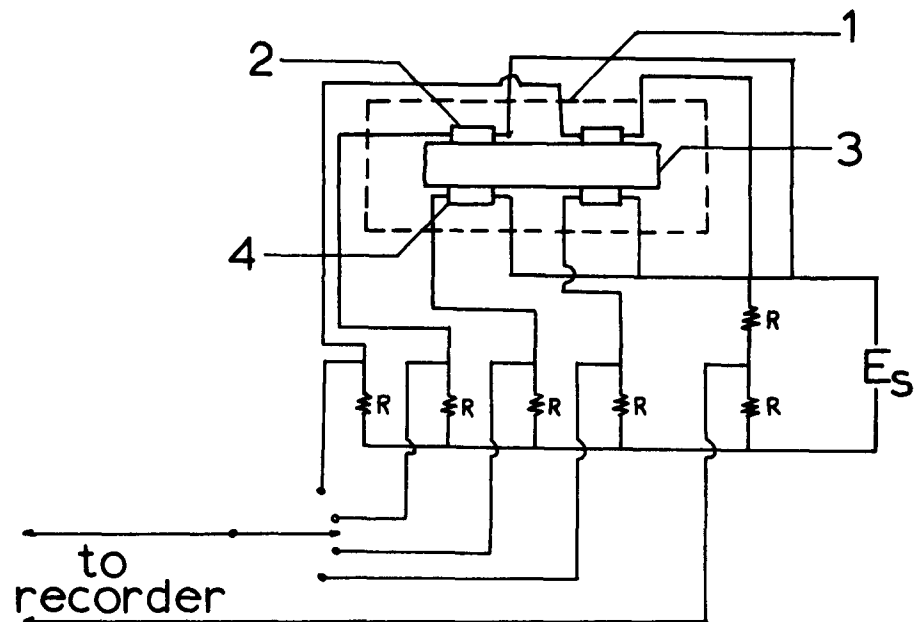
1: region near specimen
2: strain gage on upper surface
3: specimen
4: strain gage on lower surface
R: 120 precision resistors
E_S: D.C. supply voltage

Figure 20: Electrical Circuit Used with
Short Wave Case
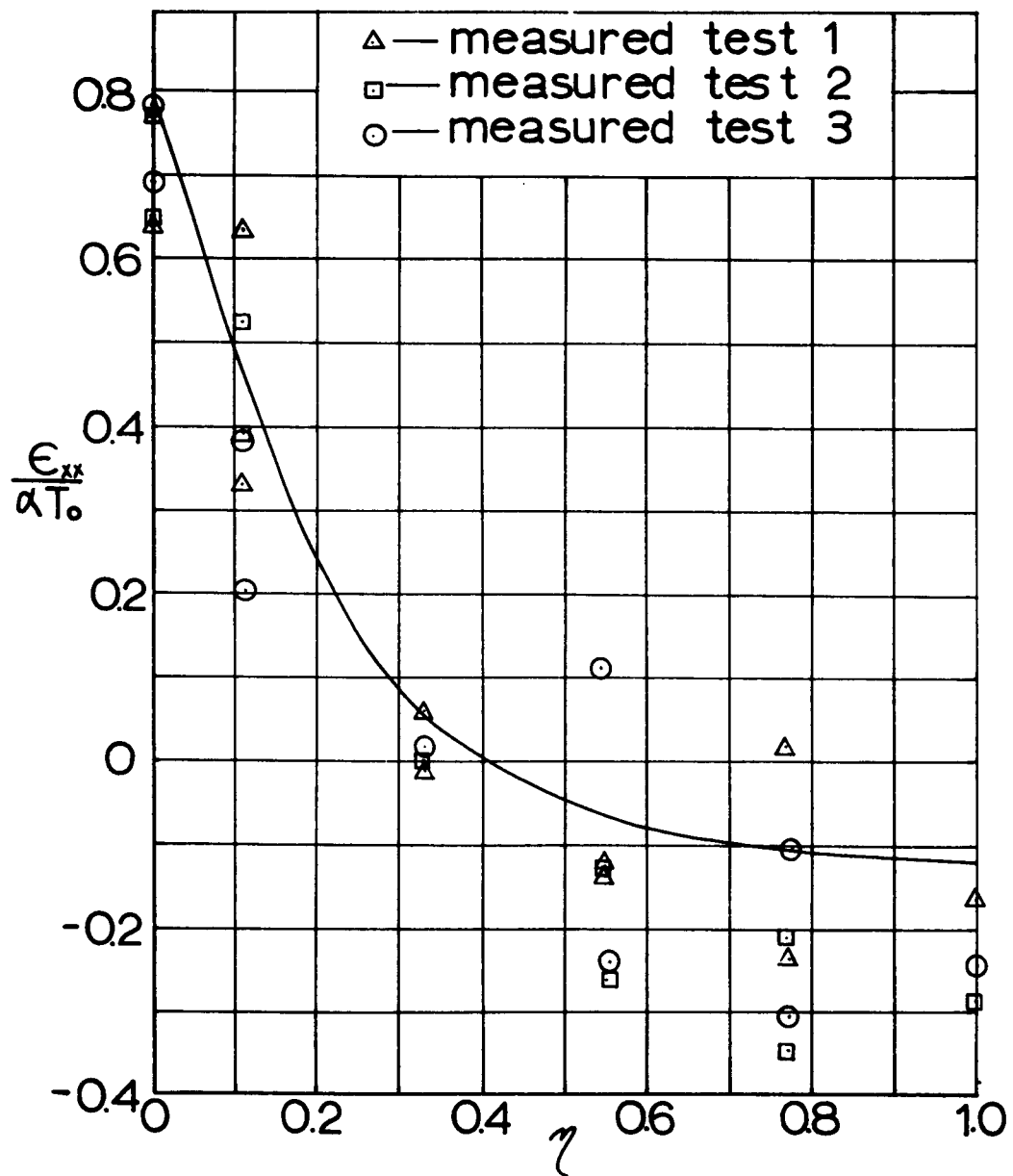
Figure 21:   Comparison of Measured Strain in
X-Direction Obtained from Four Wave
Case with Przemieniecki's Solution at
$(X/L)= 0.25$
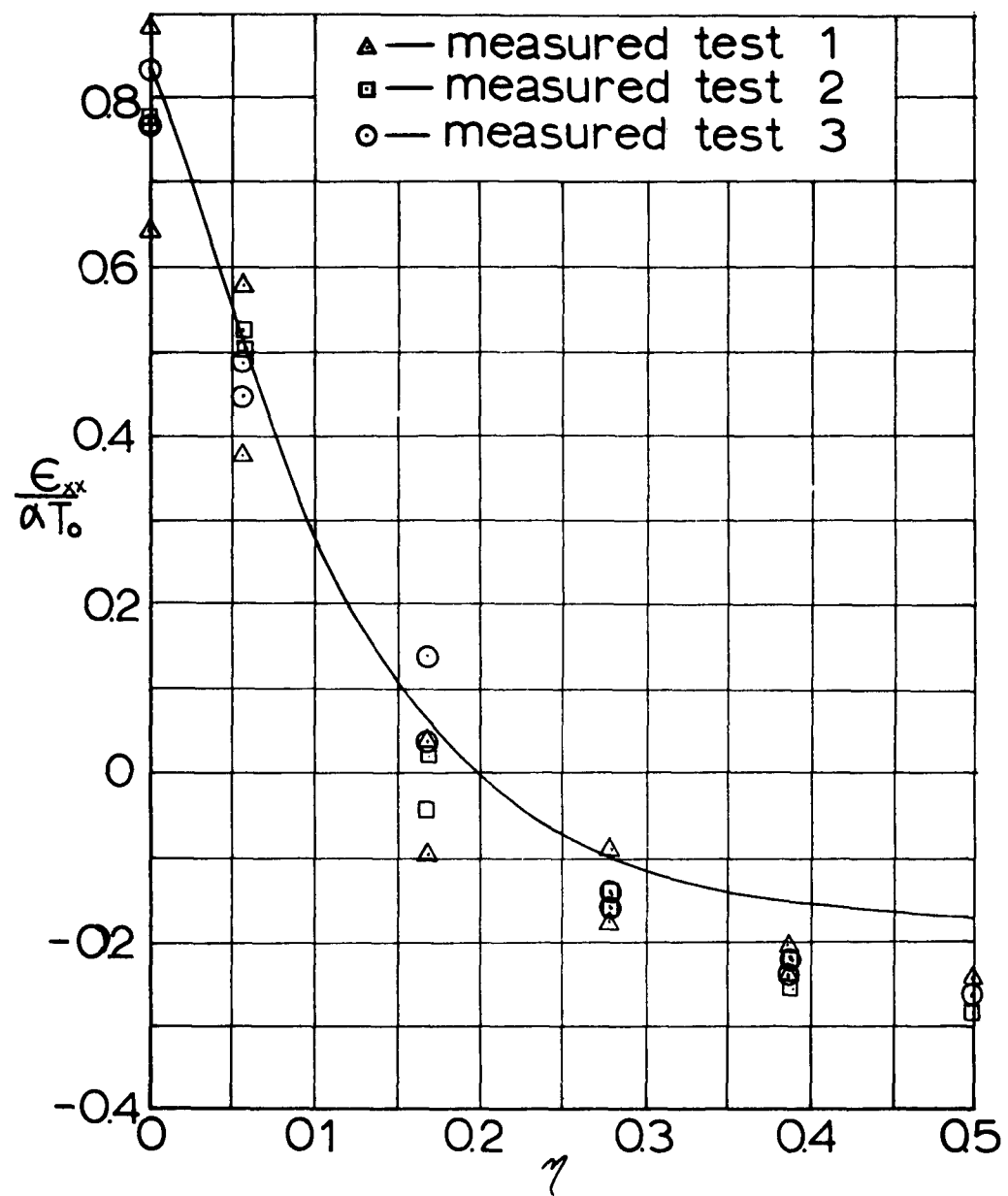
Figure 22: Comparison of Measured strain in
x-Direction Obtained from Four Wave
Case with Przemieniecki's Solution at
(X/L)= 0.75

49
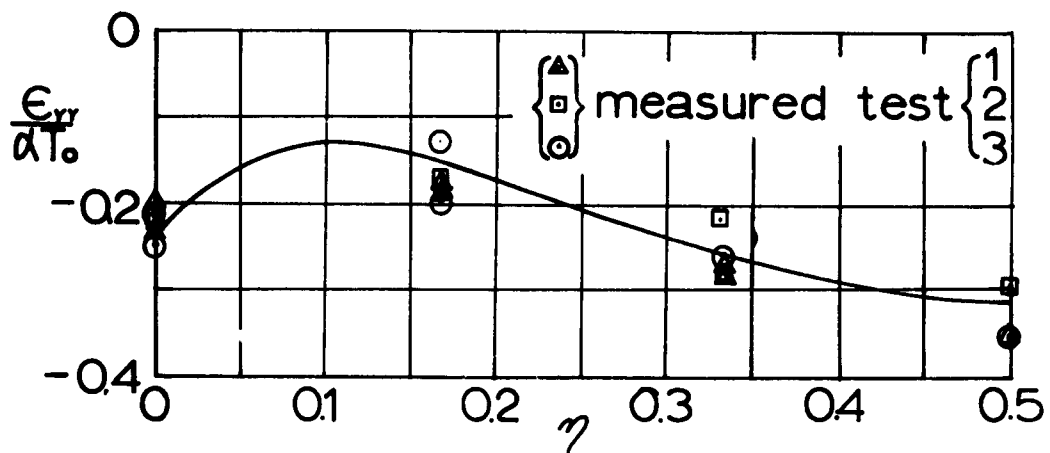
Figure 23: Comparison of Measured Strain in
Y- Direction Obtained from Four Wave
Case with Przemieniecki's Solution at
(X/L)= 0.25
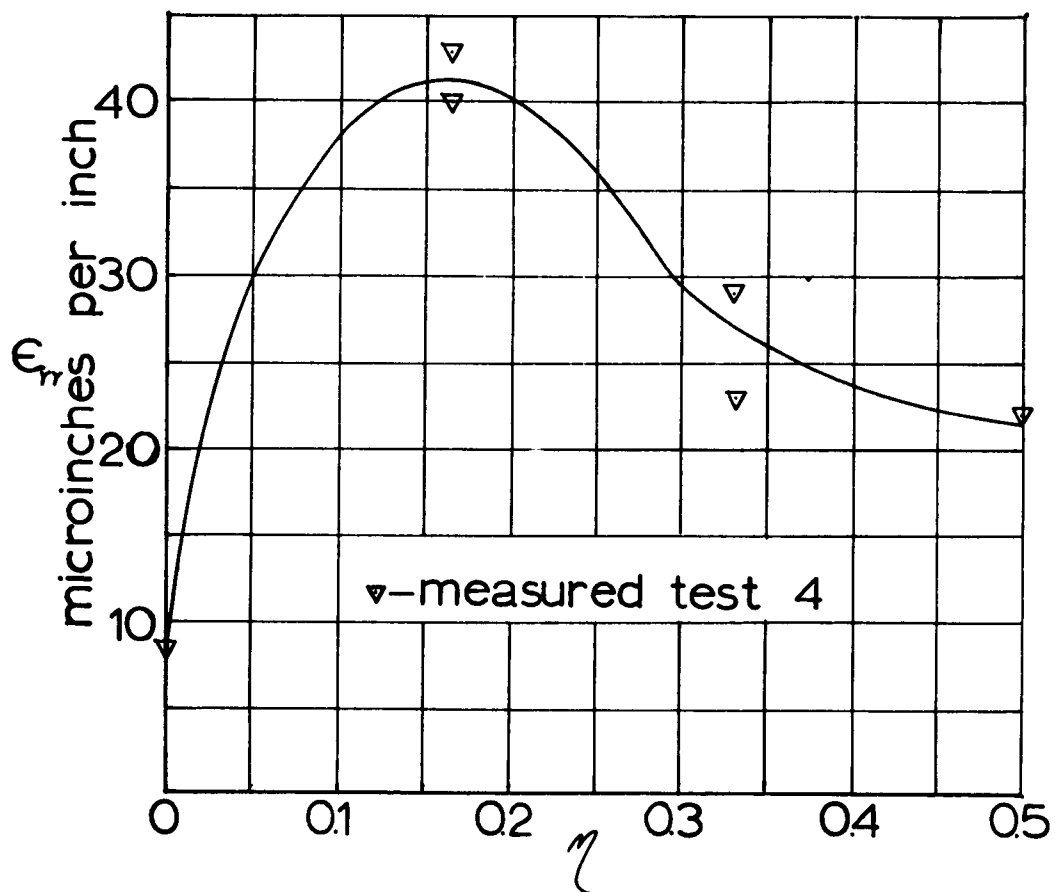
Figure 24: Measured Strain in Y- Direction at
(X/L)= 0.25; Test 4
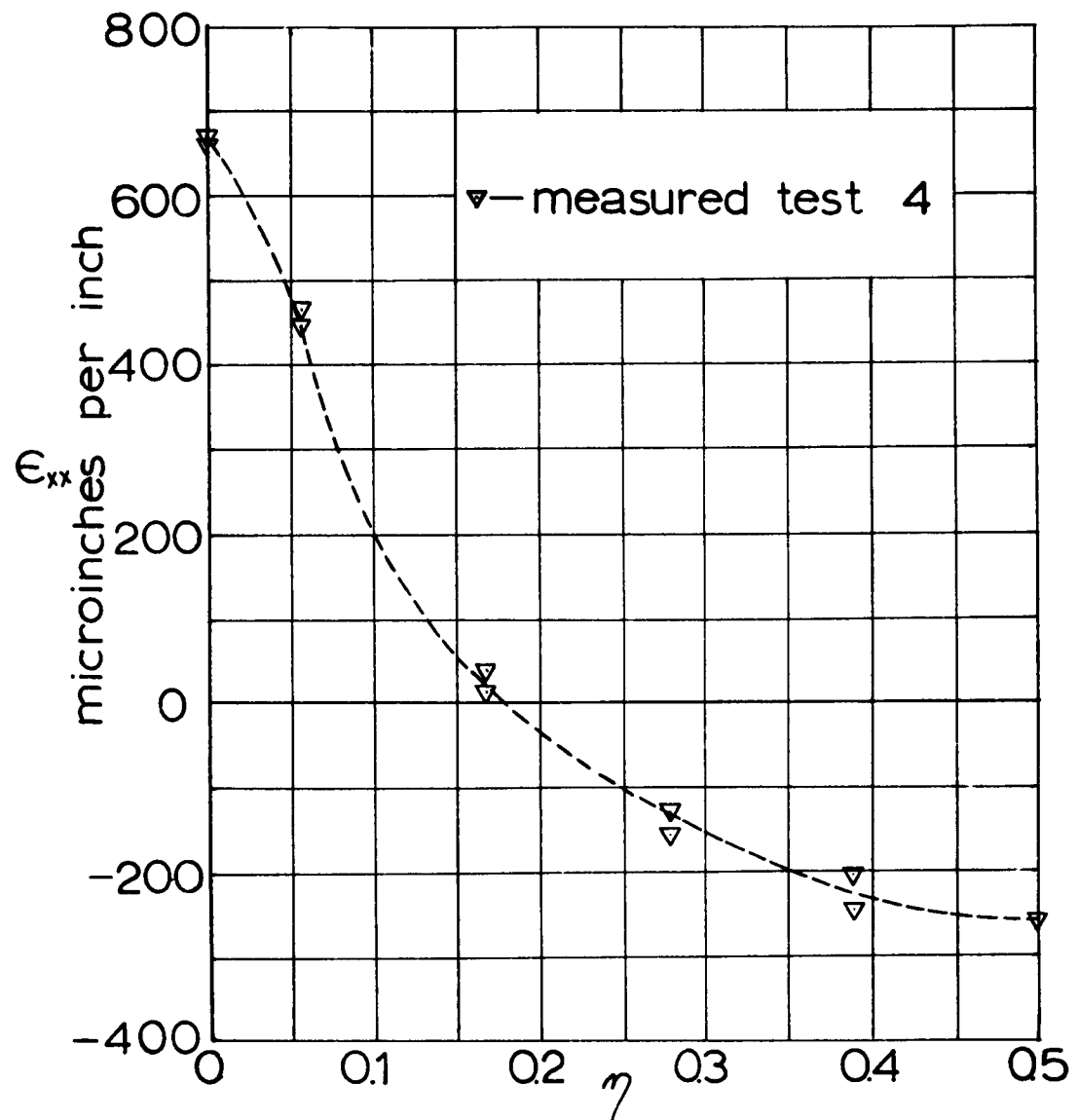
Figure 25:   Measured Strain in x- Direction at $(x/L) = 0.75$; Test 4
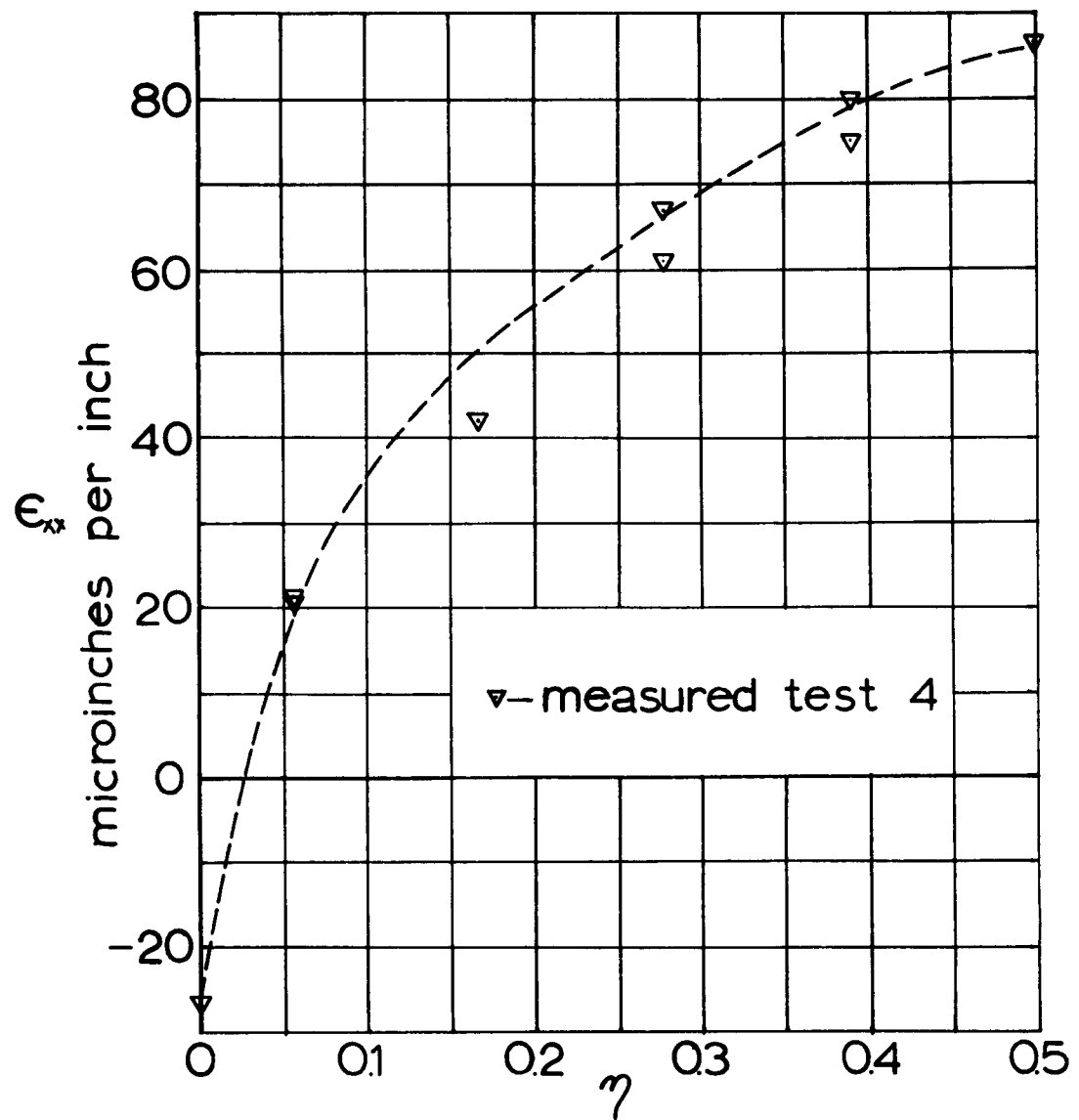
Figure 26: Measured Strain in x- Direction at (x/L)= 0.25; Test 4
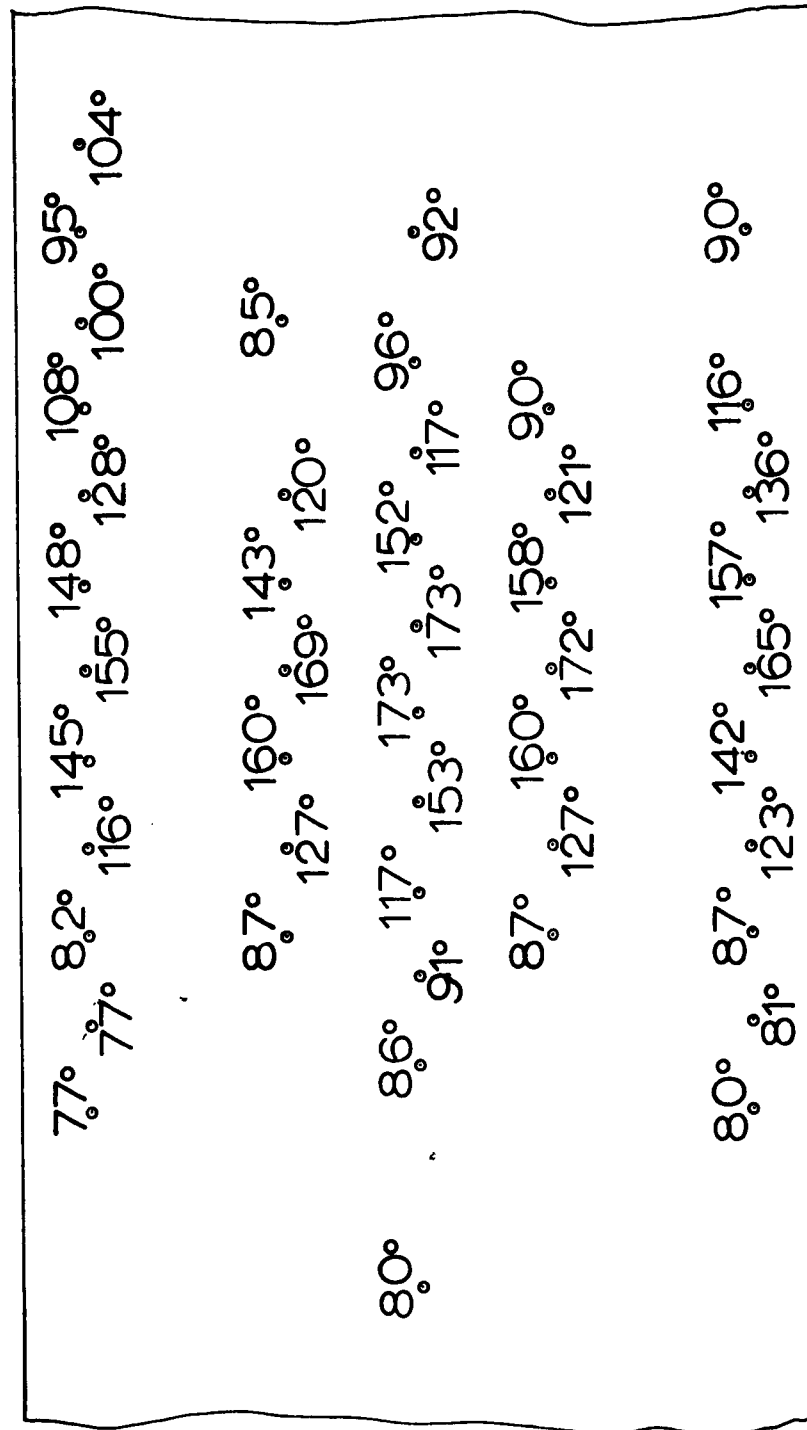
Figure 27: Measured Temperature Distribution Obtained for Short Wave Case
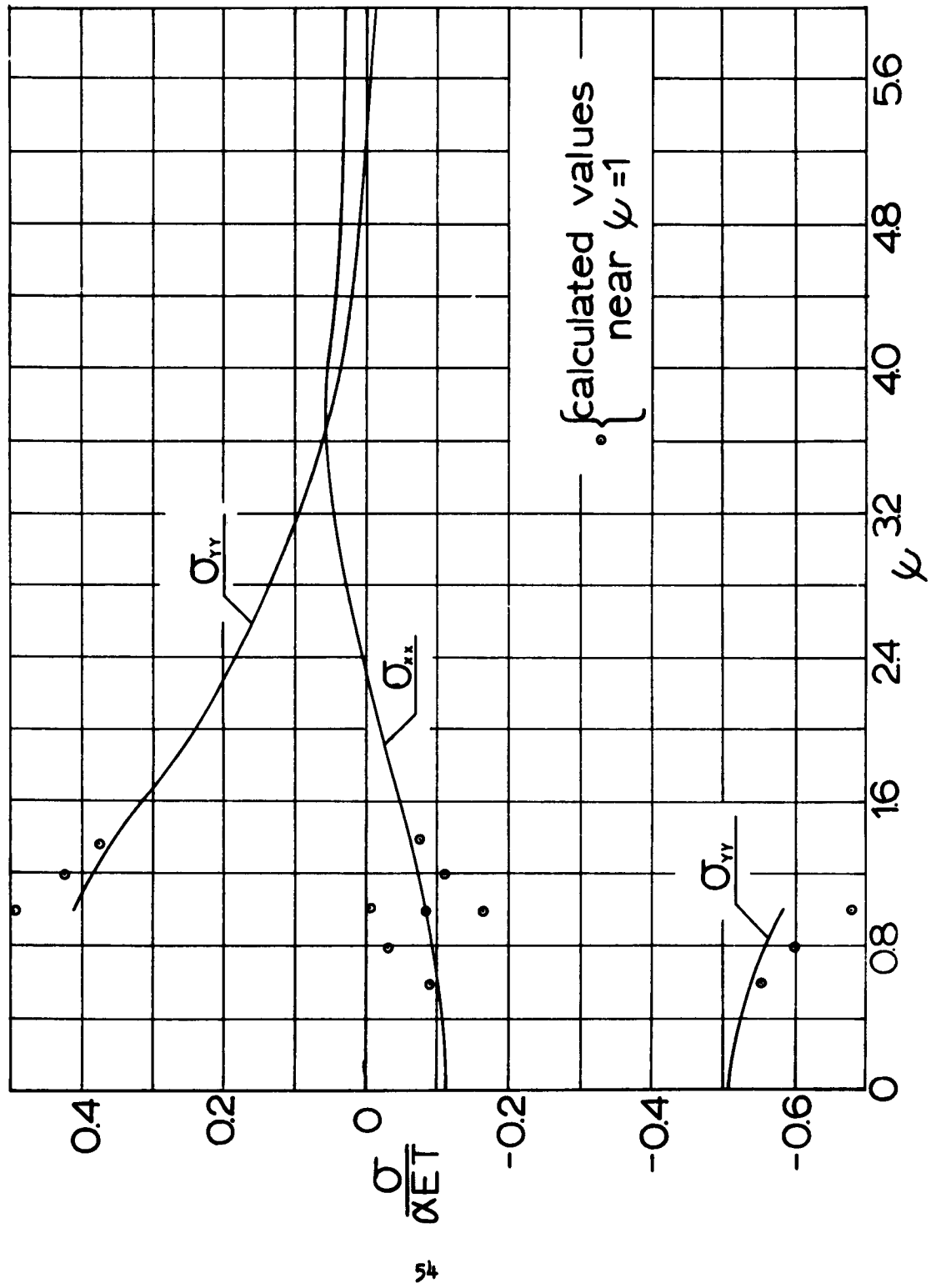
Figure 28: Calculated Stress Distribution Along
$\gamma = 0$ with $\lambda = 0.27775$
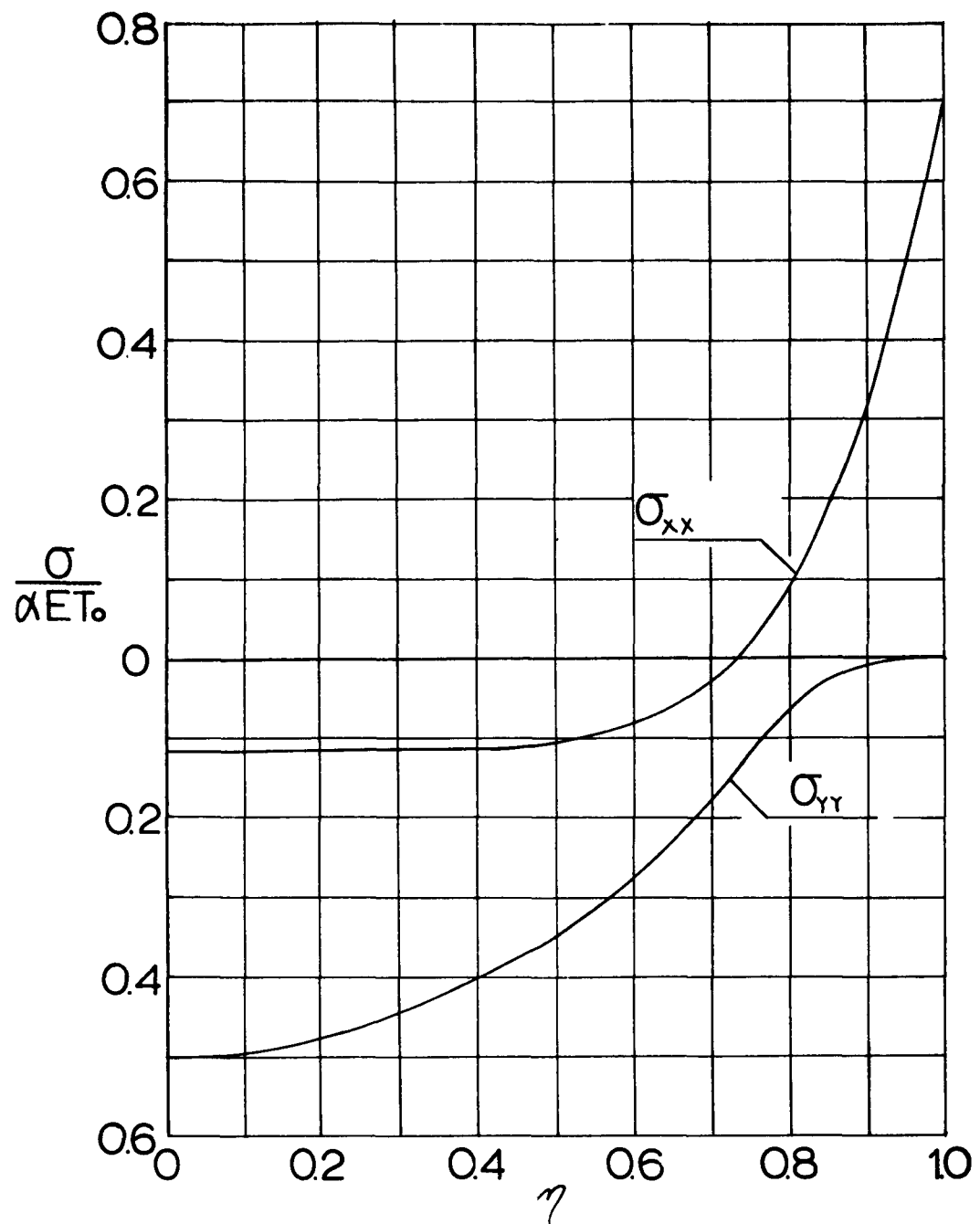
Figure 29: Calculated Stress Distribution Along
$\psi = 0$ with $\lambda = 0.27775$
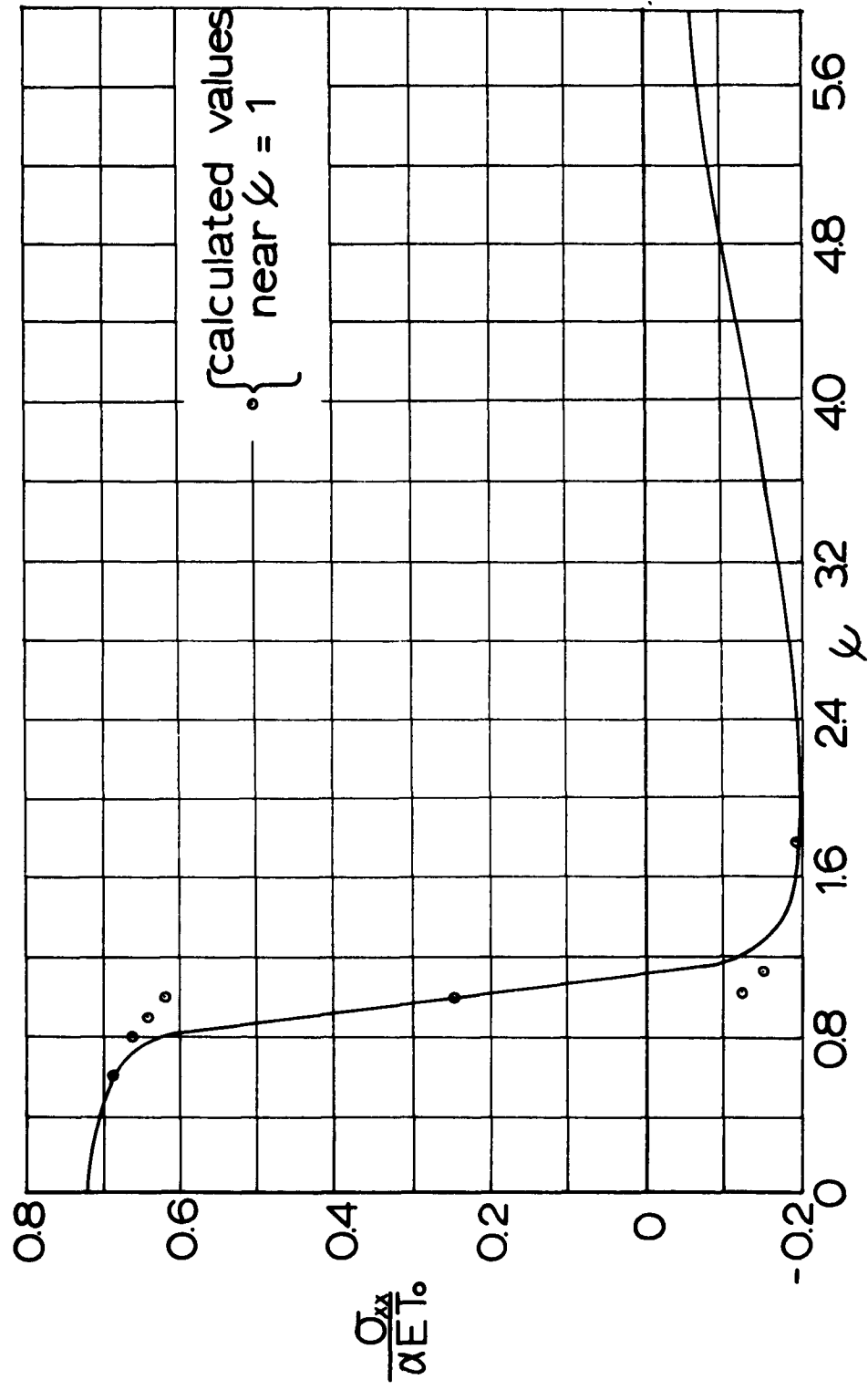
Figure 30: Calculated Stress Distribution Along
$\gamma = \pm 1$ for $\lambda = 0.27775$
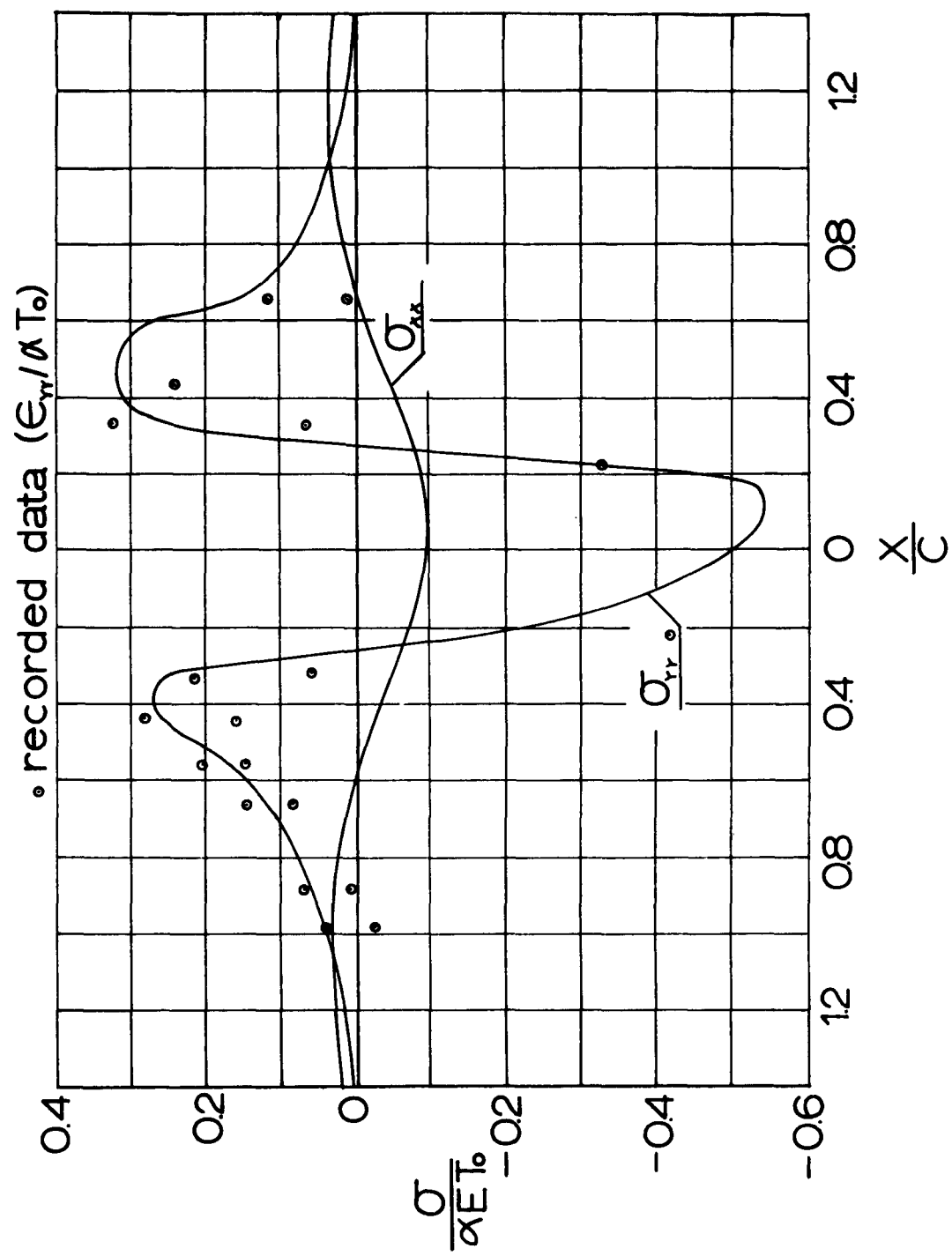
Figure 31: Calculated Stress Distribution Due
to Approximating Temperature
Distribution Along $\eta = 0$
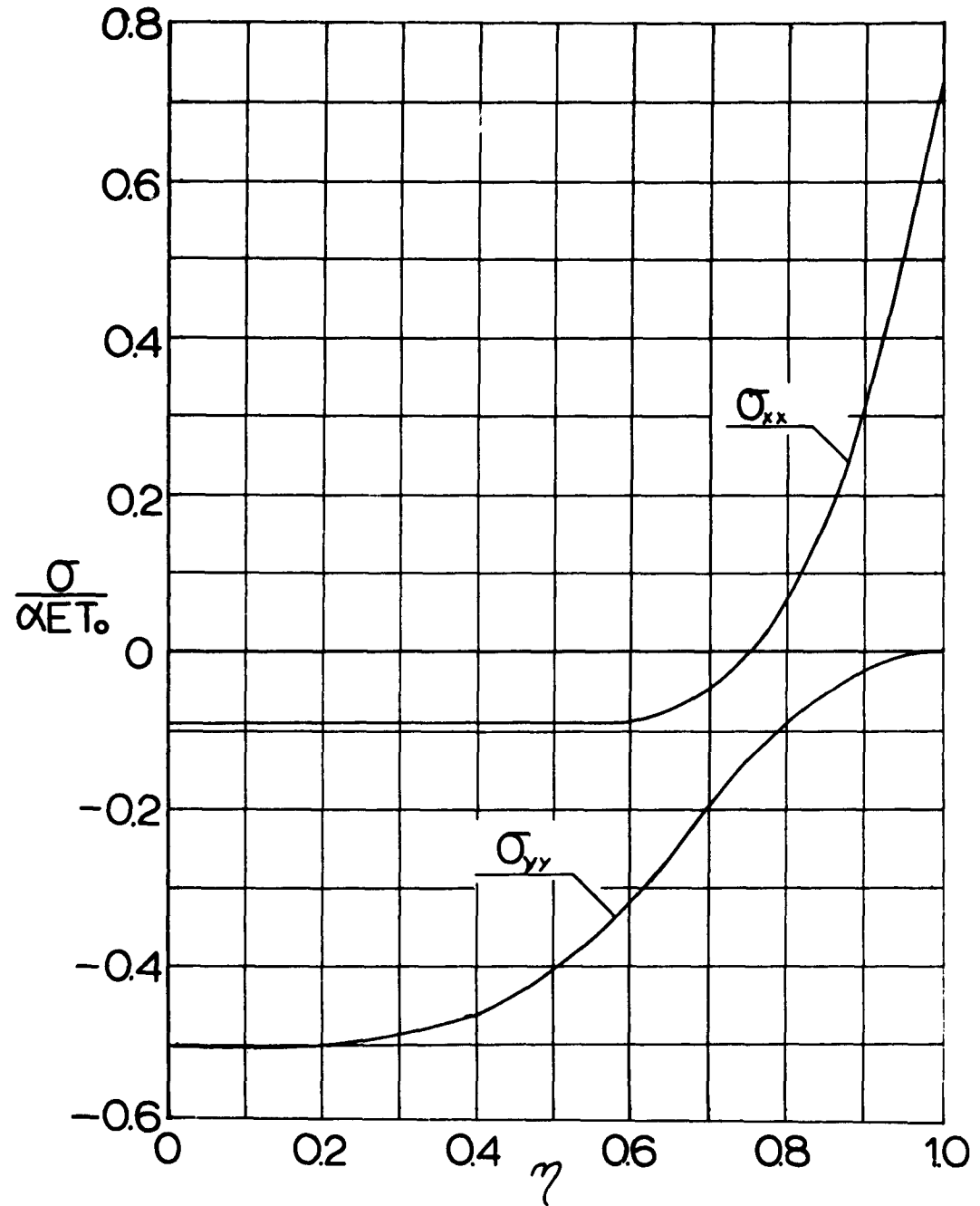
Figure 32: Calculated Stress Distribution Due
to Approximating Temperature
Distribution Along $x = 0$
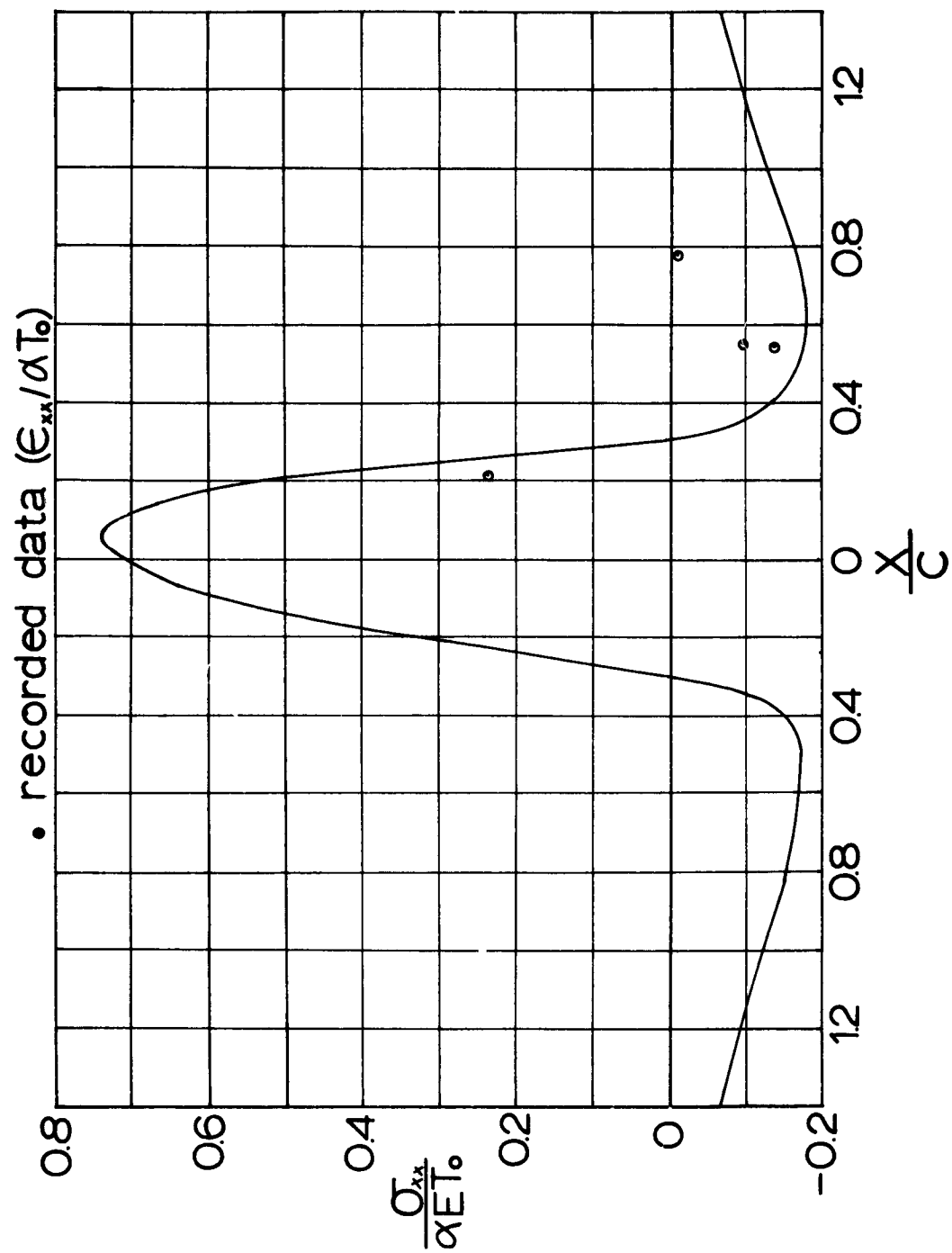
Figure 33: Calculated Stress Distribution Due
to Approximating Temperature
Distribution Along $\zeta = \pm 1$

$\frac{y}{c}$	$\frac{x}{c}=$	0	.111	.222	.333	.444	.555	.666	.777
1.000	edge	xxxxx	xxxxx	.238**	xxxxx	xxxxx	-.092**		-.247**
.943	upper	xxxxx							
	lower	.288**							
.888	upper	xxxxx			0.000**		-.107**		-.119**
	lower	xxxxx			.041**		.016**		xxxxx
.777	upper	xxxxx			-.147**				
	lower	xxxxx			+.075**				
.666	upper	xxxxx							
	lower	xxxxx							
.444	upper	xxxxx							
	lower	-.378*							
.222	upper	xxxxx							
	lower	xxxxx							
.111	upper	xxxxx							
	lower	xxxxx							
0	upper	-.031*	xxxxx	-.335*	.061*	xxxxx		-.005*	
	lower	xxxxx	xxxxx	xxxxx	.355*	.242*		.114*	
-.111	upper	xxxxx							
	lower	xxxxx							
-.222	upper	-.033*							
	lower	xxxxx							
-.444	upper	xxxxx							
	lower	xxxxx							
-.666	upper	.107*							
	lower	-.024*							
-.777	upper	.555**			.013**				
	lower	-.623**			xxxxx				
-.888	upper	xxxxx			xxxxx		-.025**		-.058**
	lower	.047**			.061**		-.315**		-.324**
-.943	upper	.641**							
	lower	xxxxx							
-1.000	edge	xxxxx	xxxxx	xxxxx	xxxxx	xxxxx	-.140**		-.012**

$\frac{y}{c}$	$\frac{x}{c}=$	-.111	-.222	-.333	-.444	-.555	-.666	-.888	-1.110
0	upper	xxxxx	xxxxx	.061*	.169*	.158*	.089*	0	-.031*
	lower	xxxxx	-.413*	.208*	.288*	.210*	.151*	.080*	.046*

* Strain measured in y-direction
** Strain measured in x-direction
All strains recorded as $\epsilon/\alpha T_o$

Figure 34: Tabular Presentation of Measured Data
for Short Wave Case
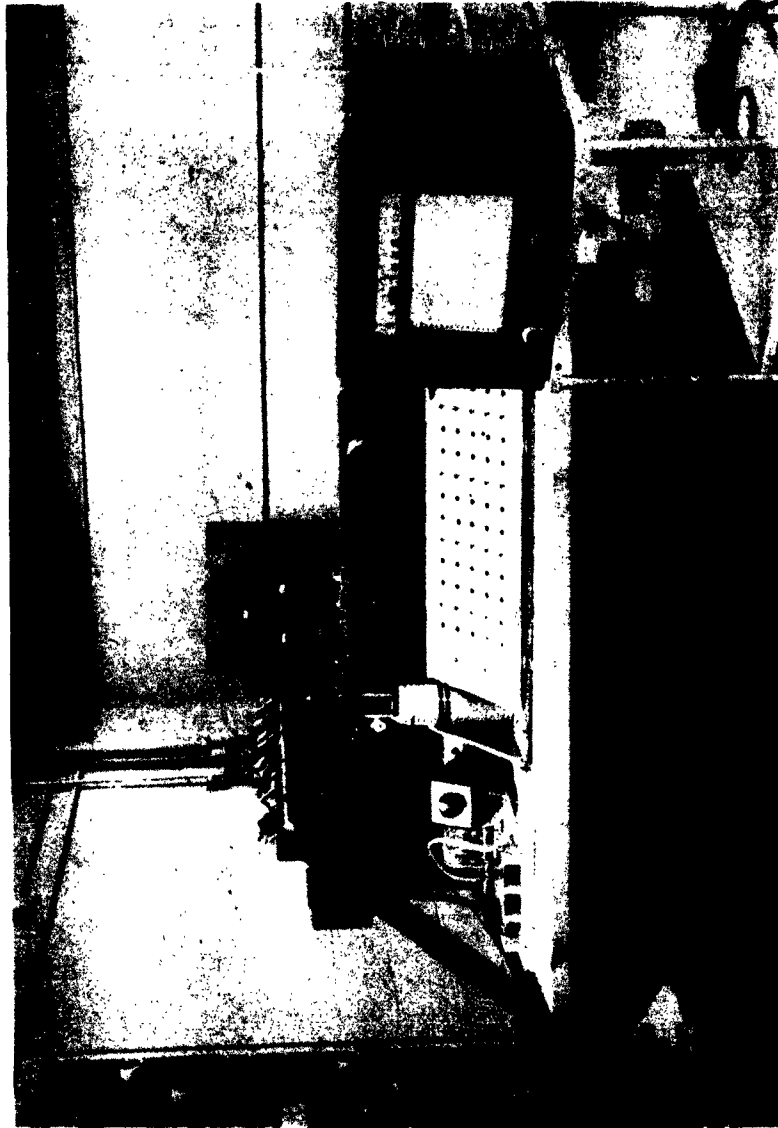
Figure 35: Photograph of Instrumentation Used for Four Wave Case
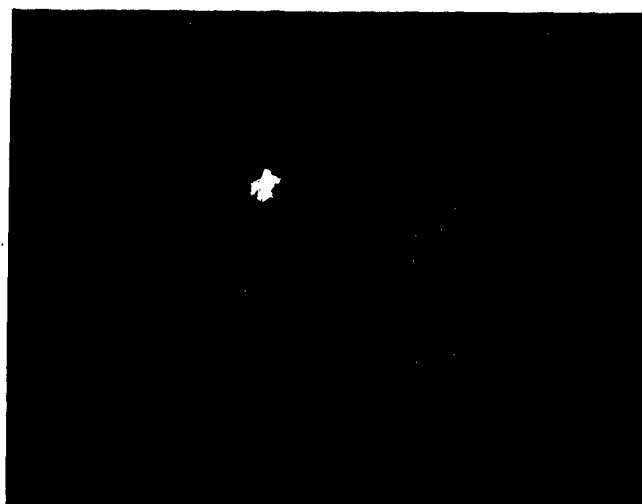
Figure 36: Photograph of Instrumentation
Used for Short Wave Case

Aeronautical Research Laboratories, Wright
Patterson AFB, Ohio. THERMAL STRESSES
DUE TO LARGE SPANWISE TEMPERATURE
GRADIENTS IN LONG THIN PLATES by B. E.
Gatewood, R. G. Dale, A. R. Glaser, The
Ohio State University, Columbus, O., Jan
uary1963. 62 p. incl. illus. (project 7063:
Task 7063-02) (Contract AF 33(616)-8330)
(ARL 63-4)   Unclassified Report

This report contains the results of a theoret-
ical and experimental investigation of the
thermal strains and stresses produced in un-
restrained long thin rectangular plates by
large spanwise temperature gradients. The
temperature distribution is steady state and
the stress distribution approximates the two-
dimensional "plane stress" solution of elas-

(over)

ticity theory. Two temperature gradients
were investigated, one which the tempera-
ture changed about 700°F over a one-inch
distance and one which the temperature
changed about 150°F over a five-inch distance.
It was found that for these relatively large
temperature gradients the solutions for the
thermal stresses given in the literature were
either not applicable or impractical because
of the large number of terms required in the
series type solutions. By converting one of
the available Fourier Series solutions into a
Fourier Integral and using residues and super-
position it is possible to construct a solution
for the stresses in which only a few terms
are needed in the series for the residues. The
calculated thermal strains compare reasona-
bly well with the experimental results, altho
there is considerable scatter in the strain
gage results on the tests.